

1 **Overpressure Transmission through Interconnected Igneous Intrusions**

2
3 **Nick Schofield¹, Simon Holford², Alex Edwards³, Niall Mark¹, Stefano Pugliese⁴**

4
5 ¹Department of Geology and Petroleum Geology, University of Aberdeen, Aberdeen AB24
6 3FX, UK

7 ²Australian School of Petroleum, University of Adelaide, Adelaide, SA 5005, Australia

8 ³Ikon Science Ltd, 1 The Crescent, Surbiton, London, KT6 4BN, UK

9 ⁴Chrysaor, Brettenham House, Lancaster Place, London WC2E 7EN

10 11 12 **Abstract**

13 In situ overpressures in sedimentary basins are commonly attributed to disequilibrium
14 compaction or fluid expansion mechanisms, though overpressures in shallow sedimentary
15 sequences may also develop by vertical transfer of pressure from deeper basin levels, for
16 example via faults. Mafic sill complexes are common features of sedimentary basins at rifted
17 continental margins, often comprising networks of interconnected sills and dikes that facilitate
18 the transfer of magma over considerable vertical distances to shallow basinal depths. Here we
19 document evidence for deep sills (depths >5 km (16,000 ft)) hosting permeable, open fracture
20 systems that may have allowed transmission of overpressure from ultra-deep basinal (>7 km
21 (23,000 ft)) levels in the Faroe-Shetland Basin (FSB), NE Atlantic Margin. Most notably, well
22 214/28-1 encountered overpressured, thin (<8 m (26 ft)) and fractured gas-charged intrusions,
23 which resulted in temporary loss of well control. While the overpressure could reflect local
24 gas generation related to thermal maturation of Cretaceous shales into which the sills were
25 emplaced, this would require the overpressures to have been sustained for unfeasibly long
26 timescales (>58 Myr). We instead suggest that transgressive, interconnected sill complexes,
27 such as those penetrated by well 214/28-1, may represent a previously unrecognized
28 mechanism of transferring overpressures (and indeed hydrocarbons) laterally and vertically
29 from deep to shallow levels in sedimentary basins, and that they represent a potentially under-

30 recognized hazard to both scientific and petroleum drilling in the vicinity of subsurface igneous
31 complexes.

32

33 **Introduction**

34 Abnormally high pore-fluid pressure, commonly referred to as overpressure, is a common
35 occurrence within sedimentary basins, occurring when the pore-fluid pressure is greater than
36 the hydrostatic pressure expected at a given depth (Neglia, 1979; Mann and Mackenzie, 1990;
37 Osborne and Swarbrick, 1997; Tingay et al., 2007). Encountering unexpected overpressure
38 zones during drilling operations can pose a significant risk to both human life, the environment
39 and a well achieving its technical objective; such zones can result in an influx of high pressure
40 gas or fluid into and up the wellbore (known as a 'kick'), and in a worst-case scenario a
41 'blowout' (Grace, 2017). Accurate prediction of pore pressures when drilling petroleum wells
42 fundamentally underlies safe drilling operations; the lack of adequate understanding and
43 subsequent response to higher than expected pore pressures during drilling of the Banjar
44 Panji-I well in Java, Indonesia was a contributing factor to the blowout and the flow of the
45 'Lusi' Mudflow, that suddenly erupted in an urban area, burying over 11,000 buildings (Tingay,
46 2015).

47 It is generally accepted that disequilibrium compaction related overpressure cannot
48 be sustained for long periods of geological time (>20 Ma) within a sedimentary basin, with the
49 overpressure dissipating via fluid leakage (Osborne and Swarbrick, 1997; Swarbrick et al.,
50 2001; Tingay et al., 2007; Luo and Vasseur, 2016). Critically, it is also generally assumed that
51 overpressure exists close to where it is generated (Osborne and Swarbrick, 1997). The
52 transfer of overpressure horizontally or vertically within sedimentary basins has not been
53 widely documented globally but with a few notable exceptions. Tingay et al. (2007)
54 demonstrated the likely vertical transfer of overpressure up normal faults within the inner

55 shelf of the Baram Delta, Borneo. Other notable areas where such pressure transfer is
56 documented is that of the Northern Carnarvon Basin, Northwest Australia Shelf (van Ruth et
57 al., 2000; Dodds et al., 2001; Tingate et al., 2001; Hoskins et al., 2015) and the Qaidam Basin,
58 northwest China (Fan et al., 2016).

59 Here we detail the occurrence of overpressure within igneous intrusions in the Faroe-
60 Shetland Basin (FSB), using a combination of subsurface datasets. We propose a new mode of
61 overpressure transfer via inter-connected networks of fractured igneous intrusions. We then
62 discuss the ramifications of such an 'overpressure' transfer mechanism for both petroleum
63 and scientific drilling in sedimentary basins containing extensive igneous intrusions (e.g. NW
64 Shelf of Australia, South Atlantic Margin, Norwegian Margin, Guaymas Basin), emphasizing the
65 need to plan for the possibility of encountering significantly higher than expected pore-fluid
66 pressures in the vicinity of igneous sheet intrusions.

67

68 **Geological History and Petroleum Exploration History of the Faroe-Shetland** 69 **Basin (FSB)**

70 The FSB is located between the Faroe Islands and Shetland Islands within the Atlantic passive
71 continental margin of NW Europe (Fig. 1). The FSB can be divided into a series of SW-NE
72 trending sub-basins and is quasi-contiguous with the Rockall Trough to the SW and the Møre
73 Basin to the NE (Hitchen and Ritchie, 1987). The sub-basins consist of Mesozoic to Recent
74 sediments bounded by basement highs comprised of Precambrian crystalline rocks capped by
75 Palaeozoic and Mesozoic sediments (Lamers and Carmichael, 1999).

76 The tectonic evolution of the FSB is complex and encompasses a number of rifting
77 phases and compressional events that span a time period of c. 400 Myr, from the Devonian
78 to the Cenozoic. Much of the present-day structure and past rifting history is thought to have
79 been heavily controlled by the NE-SW trending basement grain which formed throughout

80 NW Scotland during the Caledonian Orogeny during the Ordovician to early Devonian. The
81 first widespread phase of rifting within the basin was initiated during the Permo-Triassic, taking
82 place along the existing NE-SW Caledonian structural grain. This produced a series of half-
83 graben basins filled with fluvial, eolian and lacustrine sequences. Thermal subsidence and rising
84 global sea level led to a Lower Jurassic marine incursion (Booth et al., 1993), with thermal
85 subsidence continuing into the Middle Jurassic. Into the Upper Jurassic, the FSB underwent
86 renewed rifting, linked to the establishment of extensive rifting within the North Sea.
87 However, detailed evidence of Upper Jurassic extension within the FSB is limited by poor
88 seismic imaging beneath the Paleocene-Eocene sill complex (Schofield et al., 2015). The early
89 Cretaceous was marked by high magnitude extension as a result of the northwards
90 propagation of the Central Atlantic Rift system (Fleet and Boldy, 1999; Stoker, 2016), leading
91 to hyper-extension along the NE Atlantic Margin (Dore et al., 1997; Booth et al., 1993; Moy
92 and Imber, 2009).

93 The North Atlantic rift system became relatively inactive during the Upper
94 Cretaceous, with post-rift thermal subsidence facilitating the deposition of up to 4.5 km
95 (14,763 ft) of Upper Cretaceous sediments on the downthrown side of the major fault
96 systems. During the Paleocene, relative deepwater marine conditions existed with deposition
97 of hemi-pelagic shales and turbidite sandstones (Lamers and Carmichael 1999) as part of
98 continued post-rift thermal subsidence.

99 However, during the late Paleocene-early Eocene the FSB experienced considerable
100 igneous activity as a result of the impinging proto-Icelandic plume coinciding with continental
101 break-up of the North Atlantic (White and McKenzie, 1989). This igneous activity is expressed
102 by the eruption of extrusive basaltic sequences and the emplacement of a pervasive suite of
103 mafic sills and dykes into the sedimentary basins flanking the NE Atlantic Margin (Fig. 2) (Gibb
104 and Kanaris-Sotriou, 1998; Schofield et al., 2015). Mafic intrusions are identified throughout

105 the FSB where they are collectively termed the Faroe-Shetland Sill Complex (FSSC), and
106 extending northwards into the Møre basin and south into the Rockall Trough (Schofield et
107 al., 2017). Critically the FSSC, and the sills in other Atlantic Margin basins, are observed to
108 preferentially intrude the Cretaceous and lower Paleocene sedimentary succession, which is
109 predominantly composed of marine shales (Stoker et al., 2016) and represents a significant
110 low-permeability sealing unit (Ogilvie et al., 2015).

111 The FSB has seen active exploration for the last 50 years with the first well (206/12-
112 I) drilled in 1972 on the Rona Ridge, and over 200 exploration and appraisal wells in total
113 drilled in the FSB. Reservoirs are present throughout the entire basin succession, from
114 fractured Lewisian Gneiss crystalline basement (Lancaster Field), the fractured siliclastics in
115 the Devonian and Carboniferous Old Red Sandstone (Clair Field), Jurassic sandstones
116 (Lochnagar Discovery), Cretaceous (Victory Discovery and Edradour Field), Paleocene
117 turbidites (Schiehallion, Laggan-Tormore, Glenlivet Fields and Cragganmore Discovery),
118 Paleocene-eocene intra-basaltic fluvial deltaic sandstones (Rosebank Field), Lower Eocene
119 supra-basaltic sandstones (Cambo Field) and Mid-Eocene turbidite fan sandstones
120 (Tobermory Discovery). The majority of hydrocarbons discovered are sourced from the
121 marine Upper Jurassic Kimmeridge Clay Formation, though in some areas Middle Jurassic
122 lacustrine (Scotchman et al., 2018) and Middle Devonian lacustrine (Baron et al., 2008) sources
123 are thought to contribute.

124

125 **Overpressure Development within the Faroe-Shetland Basin**

126 Understanding the interplay of pore pressures and their impact on petroleum generation
127 during basin evolution is essential for any petroleum exploration and has particular importance
128 in the Faroe-Shetland Basin due to the tectonic complexity (Ilfie et al., 1999). Despite
129 extensive exploration activity in the FSB, a full quantitative analysis of the depth-pore pressure

130 relationships remains poorly documented in the literature. However, some broad conclusions
131 can be drawn about the pressure history of the FSB.

132 Measured reservoir pressure data show that the majority of the wells in the West of
133 Shetlands region exhibit normally pressured or near-normally pressured gradients (Iliffe et al.,
134 1999; Lamers and Carmichael, 1999; Edwards et al., 2012). However, overpressure is known
135 to occur within Mesozoic sections at depths >3,000 m (9,842 ft), with Lower Cretaceous
136 sequences generally exhibiting the largest formation overpressures (Iliffe et al., 1999; Tassone
137 et al., 2014). The distribution of overpressure within the FSB is, however, not uniform with
138 both normally pressured and overpressured high permeability sands occurring at similar
139 depths. This implies that a complex basin plumbing and fluid drainage system is in operation
140 within the FSB (Edwards et al., 2012). It is generally accepted that disequilibrium compaction,
141 as a result of high sedimentation rates in the Cenozoic, is the dominant mechanism that has
142 created the large magnitude (> 20 MPa (2,901 psi)) overpressure within the Mesozoic sections
143 of the FSB (Iliffe et al., 1999). The observation in velocity-density cross-plot space, in absence
144 of XRD-type data, show there are no deviations of data from a normal compaction trend and
145 hence, supports the notion that disequilibrium compaction is primarily active (Fig. 3). It should
146 also be noted that although the FSB has undergone multiple phases of tectonic uplift (Stoker
147 et al., 2010) the two wells of interest in this study are located in sub-basins that have
148 undergone negligible uplift, as demonstrated by Cretaceous shale compaction data (Tassone
149 et al., 2014).

150

151 **Overpressured Intrusions**

152 *Well 214/28-1 – Flett Ridge*

153 Well 214/28-1, drilled in the FSB in 1984 to a total depth of 5,124 meters below rotary table
154 (mBRT) (16,811 ft BRT) (653 m (199 ft) water depth), was designed to test Paleocene and

155 Jurassic targets (Grove, 2013). However, the well encountered substantial issues with
156 overpressured mafic intrusions between 4,596 mBRT (15,078 ft BRT) and 5,013 mBRT
157 (16,446 ft BRT) (Fig. 4), which required the expenditure of considerable time and effort to
158 control the overpressure and gas influx (Mark et al., 2017). The intrusions penetrated by Well
159 214/28-I form a series of vertically stacked intrusions that extend down towards the centre
160 of the Flett Basin and the base of the Cretaceous sequence (Schofield et al., 2015) (Fig. 2).

161 Using direct (e.g. Wireline formation tester-WFT, Repeat formation tester-RFT and
162 Modular formation dynamic tester-MDT) and indirect (e.g. mud weights), pressure data
163 indicates a consistent picture of broadly hydrostatic pressures to depth of ~3,200 m (10,498
164 ft) within the middle Paleocene (Fig. 5). Below this depth, RFT and MDT data begin to indicate
165 a departure from normal hydrostatic conditions and occurrence of overpressure, which
166 increased gradually with small deviations (e.g. 4,100 mBRT; 13,451 ft BRT). The top of
167 overpressure was estimated using intermediate wireline logs during drilling operations and
168 was found at approximately 4,480 mBRT (14,698 ft BRT) (Fig. 5). This depth is consistent with
169 regionally built shale-models in the West of Shetlands Region (Edwards et al., 2012; Tassone
170 et al., 2014). However, on encountering a 6.1 m (20 ft) thick intrusion at a sub-seabed depth
171 of 4,596 mBRT (15,075 ft BRT) (Fig. 4, 5, and 6), a large magnitude overpressure was
172 encountered associated with high pressure gas influx into the wellbore and 44% Total Gas
173 (Methane, Ethane, Propane and Butane) (Fig. 5 and 6). Using the static mud weight pressure
174 as a proxy for pore pressure in absence of direct pressure data (e.g. RFT) at this interval (van
175 Ruth et al., 2002), the circulating mud weight had to be increased to control the pore pressure
176 increase and associated gas from around 57 MPa (8,267 Psi; 10.5 ppg) to over 71 MPa (10,296
177 Psi; 13.1 ppg) (Fig. 5 and 6). On continuation of drilling, with the increased mud weight, two
178 further intrusions were penetrated at 4,788 mBRT (15,708 ft BRT) and 4,931 mBRT (16,177
179 ft BRT) respectively, with no further influx of gas noted (Fig. 6). However, at a depth of 5,013

180 mBRT (16,446 ft BRT), a 7.6 m (25 ft) thick overpressured intrusion was encountered (Fig.
181 6), with mud weights having to be raised further to counteract estimated pressure of over 82
182 MPa (11,893 Psi; 13.9 ppg). Associated with this intrusion was 51% Total Gas (Methane), which
183 when expanding at the surface led to mud flowing out over the Kelly Bushing and partial loss
184 of well control. After penetration of the 7.6 m (25 ft) thick intrusion, connection gas values
185 remained at 30-45 % even at the increased levels of mud weight to the base of hole at 5,124
186 mBRT (16,811 ft BRT).

187

188 *Well 219/28-2Z – Northern FSB*

189 Well 219/28-2Z was drilled to a total depth of 4,016 mBRT (13,175 ft BRT) (516m (1692 ft)
190 water depth) in the north east of the FSB and southern extension of the Møre Basin,
191 approximately 20 km (12 miles) northwards of the Margarita Spur. The well penetrated a 36
192 m (118 ft) thick intrusion at 3,148 mBRT (10,328 ft BRT) (~3.1 sec TWT) (Fig. 7 and 8). On
193 seismic data, the intrusion is poorly imaged due to the deep depth of imaging and inclined
194 (approximately 40°) nature of the intrusion. However, the intrusion can be seen to connect
195 sub-vertically to a series of sills intruded into the Lower Cretaceous succession. Although
196 initially, the intrusion (which was associated with a small gas peak ranging from 0.78 to 1.92%),
197 was estimated to have a pore pressure of between 39 MPa (5,706 Psi; 10.5 ppg) and 40 MPa
198 (5,923 Psi; 10.9 ppg), a direct RFT measurement taken at the lower intrusion contact gave a
199 pore pressure measurement of 48 MPa (6,956 Psi; 12.8 ppg) (Fig. 8 and 9) with the well
200 completion report noting that the high pore pressure was probably confined entirely to the
201 sill and that the adjacent claystone appeared to have been at a substantially lower pressure
202 gradient.

203

204 **Discussion**

205 **Overpressure Generation**

206 Although fluid expansion can take place by a variety of mechanisms (e.g. aquathermal
207 expansion, diagenesis; see Tingay et al., 2013), kerogen to gas maturation is generally regarded
208 as the dominant fluid expansion mechanism by which high magnitude overpressure, equivalent
209 to that formed by disequilibrium compaction can be generated (Swarbrick and Osborne, 1998;
210 Tingay et al., 2007). The emplacement of mafic, Paleogene-age intrusions into the Cretaceous
211 claystone sequences of the FSB could lead to gas generation, as a result of localized maturation
212 of organic matter by the intrusions (Aarnes et al., 2010; Muirhead et al., 2017). However, we
213 argue against this mechanism for the overpressure witnessed within the intrusions penetrated
214 in 214/28-1 and 219/28-2Z. First, multiple studies have shown that petroleum source potential
215 is generally lacking in the Cretaceous and Cenozoic stratigraphy and hence the local host
216 rocks are likely to be poor source rocks for gas (Scotchman, 2001; Scotchman, 2018). Second,
217 overpressures are inherently unstable, with pore-fluid pressures always attempting to return
218 to hydrostatic equilibrium (Osborne and Swarbrick, 1997). The residence time of
219 overpressure related to disequilibrium compaction is generally less than 20 Ma (Lou and
220 Vasseur 2016). Therefore having overpressure maintained from 58 Ma, when the sills were
221 emplaced, would exceed the generally accepted upper maximum timescale in which
222 overpressure is thought to be sustainable within most sedimentary basins.

223

224 **Fractures within Intrusions**

225 Exposed basaltic sill intrusions are often pervaded by open fractures, both vertical and
226 horizontal, in the form of cooling joints, which can create substantial fracture connectivity
227 (Bemudez and Delpino, 2008; Rateau et al., 2012; Senger et al., 2015). However, because of
228 the unloading associated with the exhumation of such intrusions to contemporary surface

229 levels, it is often difficult to assess whether open fractures visible in surface outcrops (e.g.
230 Senger et al., 2015), would still be open and interconnected in deeply buried intrusions.

231 Multiple intrusions encountered within the FSB have caused substantial mud losses
232 during drilling (Rateau et al., 2013; Mark et al., 2017). In an extreme case, 23,000 bbl of drilling
233 mud was lost into a 60 m (197 ft) thick, fractured intrusion in the FSB (208/15-1A; Mark et
234 al., 2017). In total, of the 29 wells that have encountered intrusions in the FSB, >80% have
235 suffered some degree of mud loss when drilling through intrusions (Rateau et al., 2013; Mark
236 et al., 2017).

237 Additionally, open fractures within intrusions along Atlantic Margin have been inferred
238 to control the location of oil and gas accumulations (e.g. Tormore Field), by acting as migration
239 'super-highways' through low permeability Cretaceous sequences (Rateau et al., 2013;
240 Schofield et al., 2015; Schofield et al., 2017). In Svalbard, the intrusions and surrounding
241 contact metamorphic aureoles have been inferred to control fluid flow and gas escape
242 structures adjacent to intrusions on the seafloor (Senger et al., 2013).

243 The open nature of fractures within subsurface igneous intrusions, even at depth, can
244 be substantiated directly, when available, from borehole image resistivity logs (e.g. FMI –
245 Formation Micro Imager, AFR – Azimuthal Focused Resistivity, OMRI – Oil Mud Reservoir
246 Imager). In Figure 10, a FMI log through an igneous intrusion encountered at 3,265 mBRT
247 (10,711 ft BRT) within the subsurface shows clear evidence of open horizontal and vertical
248 fractures within a 27 m (88 ft) thick intrusion. We interpret the sub-vertical fractures, which
249 extend >30° around the circumference of the hole, to be primary cooling fractures and not
250 drilling induced, as no sub-vertical fractures are seen in the weaker shale horizons above and
251 below the intrusion, and no change in mud weight occurred while drilling from the shale
252 through to the intrusion. Additionally, core obtained from intrusions within the FSB have also

253 been shown to contain open vertical and importantly horizontal natural fracture sets (i.e. not
254 induced by drilling) (Rateau et al., 2013; Grove, 2019, pers. comm.).

255 Associated with the fractures observed in the FMI log in Figure 10 is an increase in
256 separation between the logged medium and deep resistivity within the wireline logs. In the
257 areas of clear fracturing on the FMI Log (Fig. 10), the medium resistivity, which measures the
258 rock and pore fluids close to the wellbore (~1.5 m (5 ft)), is lower due to the invasion of the
259 water-based mud into the sill via the fractures (thus reducing resistivity). The deep resistivity,
260 however, remains high as it is measuring the virgin formation further away from the borehole
261 where the formation has not been invaded by the water-based mud. This same resistivity
262 separation relationship appears to be demonstrated within well 219/28-2Z, where the
263 resistivity separation within the intrusion where the elevated pore pressure was recorded by
264 the RFT can be seen clearly (Fig. 8).

265 In the case of well 214/28-1, the main evidence for presence of fractures is the
266 occurrence of the gas related 'kicks' associated with the 6.1 m (20 ft) and 7.6 m (25 ft) thick
267 intrusions (Fig. 5 and 6). As intrusions usually possess zero effective primary inter-granular
268 porosity, permeability is usually created by presence of interconnected primary or secondary
269 fractures (Bemudez and Delpino, 2008; Rateau et al., 2013).

270 Interpretation of resistivity profiles in well 214/28-1 is complicated as the section in
271 which the intrusions are present was drilled with an invert emulsion oil-based mud (IEOM).
272 Within the suite of intrusions that overpressure was encountered (Fig. 6), a clear separation
273 in resistivity is visible within two of the sills implying potential open fractures within the
274 intrusions. However, this relationship is inverse to what would be expected with an oil-based
275 mud, and therefore in the absence of image log data (which was not collected) and other
276 uncertainties (e.g. water saturation in the intrusion) it is difficult to interpret the resistivity
277 separation as being fracture-related with total confidence. Interestingly a resistivity separation

278 is not visible within the two overpressured intrusions (detailed previously). This lack of
279 resistivity separation could be the result of the drilling mud being unable to invade into the
280 fracture network of the intrusion, due to the outward force of the gas (although balanced
281 during logging), preventing the invasion of the drilling mud into fractures, thus preventing a
282 resistivity contrast.

283 The intrusions within the FSB have never been exhumed or substantially uplifted since
284 their emplacement. This suggests the fractures found in the intrusions at depth are probably
285 the result of normal cooling and contractional processes within the intrusions at the time of
286 emplacement (Bemudez and Delpino, 2008). When the fractures became open is more
287 difficult to assess and still unclear, although compressional inversion did take place within the
288 FSB from the Miocene-Oligocene, which may have reactivated existing fractures or created
289 new fractures within the intrusions (Ritchie et al., 2008).

290

291 ***'Overpressure' transmission via fractured sills***

292 Igneous intrusions within sedimentary basins often form highly interconnected complexes;
293 Cartwright and Hansen (2006) documented this phenomenon on the Norwegian Margin,
294 showing a complex of interconnected sill intrusions extending over 12 km (7.5 miles) vertically
295 and 20 km (12.4 miles) horizontally. Similar, highly interconnected complexes of mafic
296 intrusions are also observed in the FSB (Schofield et al., 2015) (Fig. 2)

297 In the specific case of the intrusions penetrated by well 214/28-1, seismic reflection
298 mapping shows that the overpressured intrusions form part of a larger, interconnected
299 intrusive complex that can be traced toward the center of the basin, 'rooting' at depths >6
300 km (19,685 ft) (Fig. 11) (Schofield et al., 2015; Mark et al. 2017). A continuous path can be
301 traced from the 6.1 m (20 ft) thick overpressured intrusion penetrated by well 214/28-1 at

302 4,596 mBRT (15,075 ft BRT), via the interconnected intrusion to over 6 km (19,685 ft) in
303 depth (Fig. 11) on 3D seismic data.

304 In well 219/28-2Z, the overpressured sill can be seen to be connected from ~3,148
305 mBRT (10,328 ft BRT), where it was penetrated by the well to a “saucer-shaped” intrusion
306 situated in the Lower Cretaceous at a depth of ~4,300 mBRT (14,108 ft BRT) (Fig. 7). The
307 saucer-shaped intrusion can be seen to be connected to a further inclined intrusion that
308 extends down to a depth of ~7 km (22,965 ft) within the Lower Cretaceous (Fig. 7).

309 Therefore, given the interconnected nature of intrusions, coupled with the evidence
310 supporting the occurrence of open fracture systems within the intrusions, it seems plausible
311 that intrusions may act as fractured conduits, hydraulically connecting separate pressure
312 regimes within a basin. This would lead to apparent ‘overpressure’ if intersected within the
313 subsurface, even though the overpressure is the result of pressure transmission from a deeper
314 sequence.

315 A common concept used to explain the presence of overpressure within reservoir
316 sand units is that of the centroid (Fig. 12) (Traugott and Heppard, 1994; Swarbrick and
317 Osborne, 1998), where lateral pressure transfer occurs through a sand body which has
318 become inclined (Swarbrick and Osborne, 1998). The centroid is the depth where the pore
319 pressure in the reservoir and bounding shale are in equilibrium, above the centroid, the pore
320 pressure in the reservoir is higher than that of the bounding shale. Below the centroid, the
321 reservoir pressure will be less than the surrounding shale (Traugott and Heppard, 1994).
322 Tingay et al. (2007) adapted this concept to illustrate that overpressures could be transferred
323 if an overpressured compartment comes into hydraulic communication with another less
324 pressured and isolated compartment either by cap-rock fracturing or active faulting.

325 In the case of the abnormally pressured intrusions within wells 214/28-1 and 219/28-
326 2Z, both suites of intrusions were penetrated by the wells situated near to the intrusion tip

327 and therefore the shallowest depth of the entire intrusive complexes, which can be seen to
328 have climbed sub-vertically, cross-cutting the stratigraphy over distances >1 km (~ 3000 ft)
329 vertically. Given the known overpressure that occurs within the shale-dominated Cretaceous
330 succession of the FSB (Illiffe et al., 1999), it seems plausible that transference of pressure is
331 occurring through the fractured intrusions, under a similar mechanism as proposed by Tingay
332 et al. (2007). However, whereas the models of Tingay et al. (2007) and others are primarily
333 concerned with generally sub-vertical to vertical transfer of overpressure, because of the
334 highly interconnected, laterally extensive nature of the intrusive complexes, overpressures in
335 the FSB could potentially be transferred laterally (and vertically) through a basin up to 10's of
336 km's away from the point of origin. Additionally, unlike the concept of the centroid, which
337 relies on recent tilting of the sand body to produce differential pressures, in the case of
338 intrusions, it is their cross-cutting nature and tendency to intrude sub-vertically which leads
339 to the pressure transfer and fluid drainage (Fig. 12).

340 It is important to acknowledge that open fracture systems within intrusions are not
341 universally prevalent within the FSB, and fractures can often be infilled by later fracture filling
342 cements (Rateau et al., 2013). Additionally, even if fractured, not all intrusions will carry
343 overpressure. Out of the 29 wells which drilled intrusions within the FSB, only two of the
344 wells, listed in this study, penetrated intrusions that had associated overpressure.

345 For an intrusion to become overpressured in the subsurface, it must satisfy several
346 criteria. It must contain an open an extensive fracture network, be connected into a deeper
347 pressure regime, and also be sealed by a suitable sealing lithology. If the intrusion intersects a
348 permeable sand sequence, the overpressure will potentially bleed off into that sequence.

349

350 ***Drilling Hazards: Are there safety and potential environmental issues with Petroleum***
351 ***and Scientific (e.g. IODP) exploration in volcanically-influenced basins?***

352 Accurate prediction of subsurface fluid pressures is a critical element of all drilling,
353 underpinning the design of safe wells (Board, 2012). Critically, pore pressure prediction
354 underpins the well design. For example, the maximum pressure tolerance of a blowout
355 preventer, and even the amount of barite and other chemicals kept on board a drilling rig to
356 enable a rapid change in mud density, are all reliant on predicting the likely pressure at a given
357 depth. In mature basins, such as the North Sea, UK, or established areas of the Gulf of Mexico,
358 where abundant primary well data exists, such prediction is generally well constrained, but in
359 frontier areas, with sparse well control, pore pressure prediction can be highly challenging.

360 Petroleum exploration wells are designed to be able to deal with (within a given
361 tolerance) excess pore pressures. However, IODP (International Ocean Drilling Program)
362 riserless drilling is conducted with no BOP and primarily using seawater as the drilling fluid,
363 meaning no primary (other than seawater) or secondary barrier exists to contain a potentially
364 overpressured zone of fluids. The risk of encountering subsurface overpressure on IODP
365 expeditions drilling is usually minimized as zones of known potential overpressure (e.g.
366 accretionary wedges; Westbrook and Smith, 1983) are avoided. Additionally, many
367 expeditions target objectives within a few hundred meters of the seabed, which can be
368 assumed to be in hydrostatic equilibrium from seabed to the eventual termination point of
369 the well. However, IODP drilling in basins effected by volcanism may be at risk from
370 intersecting sheet intrusions connected to a deeper pressure regime, especially in deeper
371 targets (>1,000 m (~ 3000 ft) below sea floor), where the strength of host rock and sealing
372 capacity may be sufficient to support overpressure connection via an interconnected intrusion
373 to a deeper pressure compartment.

374 The maximum overpressure that can occur at a given depth is reliant on the sealing
375 capacity of the host lithology in which an overpressured body is situated (Cartwright et al.,
376 2007). The most effective lithologies at containing pressure are those with low permeabilities,

377 including shales and mudstone, which sills are known to preferentially intrude (Schofield et al.,
378 2012). The maximum overpressure that can be supported by a rock unit can be expressed in
379 terms of the fracture gradient of the host rock (e.g. Fig. 4), beyond which hydraulic fracturing
380 and capillary leakage will take place and any overpressure can be assumed to dissipate.
381 Following this scenario, a well being drilled in a geological sequence containing interconnected
382 sill complexes, may have only planned to drill to a depth of e.g. 4,000 mBRT (13,123 ft BRT).
383 However, if a fractured intrusion that is part of an interconnected complex plumbed into a
384 deeper overpressure zone was penetrated, a overpressure magnitude up to the fracture
385 gradient of the host rock could be encountered (Fig. 13).

386 If during planning of the well, this scenario has not been identified, then the well design
387 may not have the inbuilt tolerances to resist the abnormal pressures, leading to a worst-case
388 scenario of a blowout, which brings a substantial risk to human life and the environment.

389

390 ***Recommendation for both Scientific (e.g. IODP) and Petroleum Drilling***

391 Sill intrusions have a fundamental underlying geological relationship in terms of thickness that
392 directly impacts on their ability to be imaged successfully using seismic reflection data. From
393 studies of both well and field data, around 60% of intrusions fall under 10m in thickness within
394 sedimentary basins globally (Button and Cawthorn, 2015, Schofield et al., 2015; Mark et al.,
395 2017; Eide et al., 2018; Svensen et al., 2018). This aspect, on its own may not appear significant,
396 but when it is considered in the context of the limitations of imaging of seismic reflection data,
397 this can become an issue. Vertical seismic resolution in seismic surveys is typically in the range
398 of 10s of meters (Cartwright et al., 2005), and at deep basin levels, e.g. 3-4 km's (9842 –
399 13,123 ft), vertical resolution can drop to 40-80 m (131 ft – 262 ft) range (Schofield et al.,
400 2015). In the case of potential pressure transmission via intrusions, this is troublesome, as it
401 means that even if intrusions cannot be confidently interpreted from seismic reflection data

402 in the vicinity of a well, they may still be present. This is illustrated in well 214/28-1, where
403 the pressure kicks emanated from intrusions that were 6.1 m (20 ft) and 7.6 m (25 ft) thick
404 respectively.

405 In areas containing pervasive subsurface intrusions, mitigating and predicting the risk
406 of which intrusions may be fractured and overpressured is challenging. Detailed seismic
407 mapping of intrusions may indicate deep connectivity, allowing some degree of mitigation
408 during the well planning phase. During drilling activities, look-ahead resistivity tools
409 (Constable et al., 2016) have the potential to alert drillers to the presence of sub-seismic
410 intrusions before they are encountered, however such tools are in a fledging stage of
411 development (Constable et al., 2016). Additionally, there is a paucity of data on the look-
412 ahead resistivity response of intrusions to permit assessment to whether an intrusion is either
413 fractured, not fractured or fractured and overpressured.

414 In both scientific and commercial drilling operations in basins affected by intrusive
415 volcanism, decisions should be underpinned by the recognition that the majority of intrusions
416 will not be visible on seismic data, and that intrusions in the region of a few meters (10's of
417 feet) are potentially capable of pressure transmission (Schofield et al., 2015; Mark et al., 2017).

418

419 **Conclusions**

420 We have detailed the occurrence of overpressure within intrusions of the FSB and propose a
421 new pathway for overpressure transfer within sedimentary basins, namely the lateral and
422 vertical transmission of pressure via vertically interconnected, fractured igneous intrusions.
423 This mechanism is previously unrecognized and may represent a significant hazard to both
424 scientific (e.g. IODP) and drilling for oil and gas in the vicinity of interconnected transgressive
425 igneous intrusive complexes in basins worldwide that contain substantial intrusive igneous

426 complexes (e.g. NW Shelf of Australia, South Atlantic Margin, Norwegian Margin, Guaymas
427 Basin)

428

429 References

- 430 Aarnes, I., Svensen, H., Connolly, J.A. and Podladchikov, Y.Y., 2010. How contact metamorphism can trigger
431 global climate changes: Modelling gas generation around igneous sills in sedimentary basins. *Geochimica*
432 *et Cosmochimica Acta*, 74(24), pp.7179-7195.
- 433 Baron, M., Parnell, J., Mark, D., Carr, A., Przyjalowski, M. and Feely, M., 2008. Evolution of hydrocarbon
434 migration style in a fractured reservoir deduced from fluid inclusion data, Clair Field, west of Shetland,
435 UK. *Marine and Petroleum Geology*, 25(2), pp.153-172.
- 436 Bermúdez, A. and Delpino, D.H., 2008. Concentric and radial joint systems within basic sills and their associated
437 porosity enhancement, Neuquén Basin, Argentina. *Geological Society, London, Special*
438 *Publications*, 302(1), pp.185-198.
- 439 Board, M., 2012, Macondo Well Deepwater Horizon Blowout: Lessons for Improving Offshore Drilling Safety.
440 National Academies Press.
- 441 Booth, J., Swiecicki, T. and Wilcockson, P., 1993, January. The tectono-stratigraphy of the Solan Basin, west of
442 Shetland. In *Geological Society, London, Petroleum Geology Conference series* (Vol. 4, No. 1, pp. 987-998).
443 Geological Society of London.
- 444 Bowers, G., 1994, Pore pressure estimation from velocity data: accounting for overpressure mechanisms besides
445 undercompaction. *Society of Petroleum Engineers Paper 27488*, International Association of Drilling
446 Contractors/Society of Petroleum Engineers Drilling Conference: Dallas, p. 515-530.
- 447 Bowers, G.L., 1995, Pore pressure estimation from velocity data: Accounting for overpressure mechanisms
448 besides undercompaction: *SPE Drilling and Completion*, v. 10, p. 89-95.
- 449 Button, A., and R. G. Cawthorn. "Distribution of mafic sills in the Transvaal Supergroup, northeastern South
450 Africa." *Journal of the Geological Society* 172.3 (2015): 357-367.
- 451 Cartwright, J., & Huuse, M. (2005). 3D seismic technology: the geological 'Hubble'. *Basin Research*, 17(1), 1-20.
- 452 Cartwright, J. and Møller Hansen, D., 2006. Magma transport through the crust via interconnected sill
453 complexes. *Geology*, 34(11), pp.929-932.
- 454 Cartwright, J., Huuse, M. and Aplin, A., 2007. Seal bypass systems. *AAPG bulletin*, 91(8), pp.1141-1166.
- 455 Constable, M. V., Antonsen, F., Stalheim, S. O., Olsen, P. A., Fjell, O. Z., Dray, N. Tan, S. (2016, October 1).
456 Looking Ahead of the Bit While Drilling: From Vision to Reality. *Society of Petrophysicists and Well-Log*
457 *Analysts*.
- 458 Deming, D., 1994. Factors necessary to define a pressure seal. *AAPG bulletin*, 78(6), pp.1005-1009.
- 459 Dodds, K., Flecher, A., Bekele, E.b. Hennig, A.L., Johnson, M. D. Abriel, W., Higgs, W.G. and Strudley, A. 2001.
460 An overpressure case history using a novel risk analysis process. *APPEA Journal* 559-571.
- 461 Doré, A.G., Lundin, E.R., Fichler, C. and Olesen, O., 1997. Patterns of basement structure and reactivation along
462 the NE Atlantic margin. *Journal of the Geological Society*, 154(1), pp.85-92.
- 463 Edwards, A., O'Connor, S., Kelly, P., Heller, J., Odesanya, F., Green, S., Hoskin, E., and Diaz, M. The West of
464 Shetlands Regional Pressure Study. Non-proprietary regional study.
- 465 Edwards, A., O'Connor, S., Swarbrick, R., Alderson, A. and Diaz, M. 2012. Overpressure mapping in the West
466 of Shetlands Basin. Abstract, PETEX, London.
- 467 Eide, C.H., Schofield, N., Lecomte, I., Buckley, S.J. and Howell, J.A., 2018. Seismic interpretation of sill complexes
468 in sedimentary basins: implications for the sub-sill imaging problem. *Journal of the Geological Society*, 175(2),
469 pp.193-209.
- 470 Ellis, D., Jolley, D. W., Passey, S. R. & Bell, B. R. 2009. Transfer zones: The application of new geological
471 information from the Faroe Islands applied to the offshore exploration of intra basalt and sub-
472 basalt strata. In: Varming, T. & Ziska, H (eds) *Faroe Islands Exploration Conference: Proceedings of*
473 *the 2nd conference. Annals Societatis Scientiarum Faerensis, Supplementum. 50, 205-226.*

- 474 Fan, C., Wang, Z., Wang, A., Fu, S., Wang, L., Zhang, Y., Kong, H. and Zhang, X., 2016. Identification and
475 calculation of transfer overpressure in the northern Qaidam Basin, northwest China. *AAPG*
476 *Bulletin*, 100(1), pp.23-39.
- 477 Fleet, A. J., & Boldy, S. A. (Eds.). (1999). *Petroleum geology of northwest Europe: Proceedings of the 5th*
478 *Conference*. Geological Society of London.
- 479 Gibb, F.G.F. and Kanaris-Sotiriou, R., 1988. The geochemistry and origin of the Faeroe-Shetland sill
480 complex. Geological Society, London, Special Publications, 39(1), pp.241-252.
- 481 Grace, R.D., 2017. *Blowout and well control handbook*. Gulf Professional Publishing.
- 482 Grauls, D.J., and Baleix, J.M., 1994, Role of overpressures and in situ stresses in fault-controlled hydrocarbon
483 migration: A case study: *Marine and Petroleum Geology*, v. 11, p. 734–742, doi: 10.1016/0264-
484 8172(94)90026-4.
- 485 Grant, N., Bouma, A., and McIntyre, A. 1999. The Turonian play in the Faeroe-Shetland basin, in Fleet, A.J. and
486 Boldy, S.A.R. eds., *Petroleum Geology of Northwest Europe: Proceedings of the 5th Conference*, London,
487 The geological Society, London, 661-673.
- 488 Grove, C., 2013. Submarine hydrothermal vent complexes in the Paleocene of the Faeroe-Shetland Basin: Insights
489 from three-dimensional seismic and petrographical data. *Geology*, 41(1), pp.71-74.
- 490 Hardman, J. P. A., Schofield, N., Jolley, D. W., Holford, S. P., Hartley, A. J., Morse, S., Underhill, J. R.,
491 Watson, D. A. & Zimmer, E. H. 2018a. Prolonged dynamic support from the Icelandic plume of the
492 NE Atlantic Margin. *Journal of the Geological Society*, London. First Published Online:
493 <https://doi.org/10.1144/jgs2017-088>
- 494 Hardman, J., Schofield, N., Jolley, D., Hartley, A., Holford, S. & Watson, D. 2018b. Controls on the
495 distribution of volcanism and intra-basaltic sediments in the Cambo-Rosebank region, West of
496 Shetland. *Petroleum Geoscience*, First Published Online: [https://doi.org/10.1144/petgeo2017-](https://doi.org/10.1144/petgeo2017-061)
497 [061](https://doi.org/10.1144/petgeo2017-061)
- 498 Hitchen, K. and Ritchie, J.D., 1987. Geological review of the West Shetland area. *Petroleum Geology of North West*
499 *Europe*. Graham & Trotman, London, 737, p.749.
- 500 Hoskins, E., O'Connor, S., Robertson, S., Streit, J., Ward, C., Lee, J. and Flett, D. Influence of faulting on reservoir
501 overpressure distribution in the Northern Carnarvon Basin. *APPEA Journal*, 1-13.
- 502 Illife, J.E., Robertson, A.G., Ward, G.H.F., Wynn, C., Pead, S.D.M., and Cameron, N. 1999. The importance of
503 fluid pressures and migration to the hydrocarbon prospectivity of the Faeroe-Shetland White Xone, in Fleet,
504 A.J. and Boldy, S.A.R. eds., *Petroleum Geology of Northwest Europe: Proceedings of the 5th Conference*,
505 London, The geological Society, London, 601-611.
- 506 Lahann, R.W., McCarty, D., and Hsieh, J., 2001, Influence of Clay Diagenesis on Shale Velocities and Fluid
507 Pressure, *Offshore Technology Conference (OTC 13046)*.
- 508 Lamers, E., and Carmichael, S.M.M. 1999. The Paleocene deepwater sandstone play of West of Shetlands, in
509 Fleet, A.J. and Boldy, S.A.R. eds., *Petroleum Geology of Northwest Europe: Proceedings of the 5th*
510 *Conference*, London, The geological Society, London, 645-659.
- 511 Luo, X. and Vasseur, G. 2016. Overpressure dissipation mechanisms in sedimentary sections consisting of
512 alternating mud-sand layers. *Marine and Petroleum Geoscience*, 78 883-894.
- 513 Mann, D.M. and Mackenzie, A.S., 1990. Prediction of pore fluid pressures in sedimentary basins. *Marine and*
514 *Petroleum Geology*, 7(1), pp.55-65.
- 515 Mark, N.J., Schofield, N., Pugliese, S., Watson, D., Holford, S., Muirhead, D., Brown, R. and Healy, D. (2017)
516 'Igneous intrusions in the Faeroe Shetland basin and their implications for hydrocarbon exploration: new
517 insights from well and seismic data'. *Marine and Petroleum*
518 *Geology*. DOI: 10.1016/j.MARPETGEO.2017.12.005
- 519 Moy, D.J. and Imber, J., 2009. A critical analysis of the structure and tectonic significance of rift-oblique
520 lineaments ('transfer zones') in the Mesozoic–Cenozoic succession of the Faeroe–Shetland Basin,
521 NE Atlantic margin. *Journal of the Geological Society*, 166(5), pp.831-844.
- 522 Mudge, D. C. 2014. Regional controls on Lower Tertiary sandstone distribution in the North Sea and NE
523 Atlantic margin basins. In: McKie, T. Rose, P. T. S. Hartley, A. J. Jones, D. W. & Armstrong, T. L.
524 (eds) *Tertiary Deep-Marine Reservoirs of the North Sea Region*. Geological Society, London,
525 *Special Publications*, 403, 17-42.

- 526 Neglia, S., 1979. Migration of fluids in sedimentary basins. *AAPG Bulletin*, 63(4), pp.573-597.
- 527 Ogilvie, S., Barr, D., Roylance, P. and Dorling, M., 2015. Structural geology and well planning in the Clair
528 Field. Geological Society, London, Special Publications, 421(1), pp.197-212.
- 529 Osborne, M.J. and Swarbrick, R.E., 1997. Mechanisms for generating overpressure in sedimentary basins: A
530 reevaluation. *AAPG bulletin*, 81(6), pp.1023-1041.
- 531 Rateau, R., Schofield, N. and Smith, M., 2013. The potential role of igneous intrusions on hydrocarbon migration,
532 West of Shetland. *Petroleum Geoscience*, 19(3), pp.259-272.
- 533 Rider, M., Kennedy, M., 2011. *The Geological Interpretation of Well Logs*, third ed. Rider-
534 French Consulting Ltd, Glasgow.
- 535 Ritchie, J.D., Johnson, H., Quinn, M.F. and Gatliff, R.W., 2008. The effects of Cenozoic compression within the
536 Faroe-Shetland Basin and adjacent areas. Geological Society, London, Special Publications, 306(1),
537 pp.121-136.
- 538 Ritchie, J.D., Ziska, H., Johnson, H. and Evans, D., 2011. Geology of the Faroe-Shetland Basin and adjacent areas.
- 539 Ruth P.J. van , Hillis R.R. Swarbrick R.E., 2002, Detecting overpressure using porosity-based techniques in the
540 Carnarvon Basin, Australia. *The APPEA Journal* 42, 559-569.
- 541 Schofield, N.J., Brown, D.J., Magee, C. and Stevenson, C.T., 2012. Sill morphology and comparison of brittle and
542 non-brittle emplacement mechanisms. *Journal of the Geological Society*, 169(2), pp.127-141.
- 543 Schofield, N., Holford, S., Millet, J., Brown, D., Jolley, D., Passey, S.R., Muirhead, D., Grove, C., Magee, C., Murray,
544 J., Hole, M., Jackson, C.A.-L., Stevenson, C., 2015. Regional magma plumbing and emplacement
545 mechanisms of the Faroe-Shetland Sill Complex: implications for magma transport and petroleum systems
546 within sedimentary basins. *Basin Res.* 19. <http://doi.org/10.1111/bre.12164>.
- 547 Schofield, N., Jolley, D., Holford, S., Archer, S., Watson, D., Hartley, A., Howell, J., Muirhead, D., Underhill, J.,
548 Green, P., 2017, Challenges of future exploration within the UK Rockall Basin. In: *Geological Society*,
549 London, *Petroleum Geology Conference Series*, vol. 8. Geological Society of London, pp. PGC8–37.
- 550 Scotchman, I. 2001. Petroleum geochemistry of the Lower and Middle Jurassic in Atlantic margin basins of Ireland
551 and the UK. In: Shannon, P.M., Haughton, P.D.W. & Corcoran, D.V. (eds). *The petroleum exploration of*
552 *Ireland's Offshore Basins*, Geological Society of London, London, Special Publications 188, 31-60.
- 553 Scotchman, I.C., Doré, A.G. and Spencer, A.M., 2018, January. Petroleum systems and results of exploration on
554 the Atlantic margins of the UK, Faroes & Ireland: what have we learnt?. In *Geological Society, London,*
555 *Petroleum Geology Conference series* (Vol. 8, No. 1, pp. 187-197). Geological Society of London.
- 556 Senger, Kim, et al. "Geometries of doleritic intrusions in central Spitsbergen, Svalbard: an integrated study of an
557 onshore-offshore magmatic province with implications for CO₂ sequestration." *Geological controls on*
558 *fluid flow and seepage in western Svalbard fjords, Norway. An integrated marine acoustic study* (2013).
- 559 Senger, K., Buckley, S.J., Chevallier, L., Fagereng, Å., Galland, O., Kurz, T.H., Ogata, K., Planke, S. and Tveranger,
560 J., 2015. Fracturing of doleritic intrusions and associated contact zones: Implications for fluid flow in
561 volcanic basins. *Journal of African Earth Sciences*, 102, pp.70-85.
- 562 Stoker, M.S. 2016. Cretaceous tectonostratigraphy of the Faroe–Shetland region. *Scottish Journal of Geology*,
563 <https://doi.org/10.1144/sjg2016-004>
- 564 Stoker, M.S., Holford, S.P., Hillis, R.R., Green, P.F. and Duddy, I.R., 2010, Cenozoic post-rift sedimentation off
565 northwest Britain: Recording the detritus of episodic uplift on a passive continental margin. *Geology*, 38,
566 595-598.
- 567 Swarbrick, R.E., Osborne, M.J. and Yardley, G.S., 2001, *AAPG Memoir 76*, Chapter 1: Comparison of
568 Overpressure Magnitude Resulting from the Main Generating Mechanisms.
- 569 Svensen, H. H., Polteau, S., Cawthorn, G., & Planke, S. (2018). Sub-volcanic intrusions in the Karoo basin, South
570 Africa. In *Physical Geology of Shallow Magmatic Systems* (pp. 349-362). Springer, Cham.
- 571 Tassone, D.R., Holford, S.P., Stoker, M.S., Greem P., Johnson, H., Underhill, J.R. and Hillis, R.R. 2014.
572 Constraining Cenozoic exhumation in the Faroe-Shetland region using sonic transit time data. *Basin*
573 *Research*, 26, 38-72.
- 574 Tingate, P.R., Khaksar, A., van Ruth, P., Dewhurst, D.N., Raven, M.D., Young, H., Hillis, R. R., and Dodds, K.
575 2001. Geological controls on overpressure in the Northern Carnarvon Basin. *APPEA Journal* 573-593.

- 576 Tingay, M.R., Hillis, R.R., Swarbrick, R.E., Morley, C.K. and Damit, A.R., 2007, 'Vertically
577 transferred' overpressures in Brunei: Evidence for a new mechanism for the formation of high-magnitude
578 overpressure. *Geology*, 35(11), pp.1023-1026
- 579 Tingay, M.R., Morley, C.K., Laird, A., Limpornpipat, O., Krisadasima, K., Pabchanda, S. and Macintyre, H.R., 2013.
580 Evidence for overpressure generation by kerogen-to-gas maturation in the northern Malay Basin. *AAPG*
581 *bulletin*, 97(4), pp.639-672.
- 582 Tingay, 2015, Initial pore pressures under the Lusi mud volcano, Indonesia. *Interpretation*, 3, 33-49.
- 583 Traugott, Martin O., and Phillip D. Heppard. "Prediction of pore pressure before and after drilling—Taking the
584 risk out of drilling overpressured prospects." AAPG Hedberg Research Conference. Vol. 70. 1994.
- 585 Van Ruth, P.J., Hillis, R.R., Swarbrick, R. and Tingate, P. 2000. Mud weights, transient pressure tests and the
586 distribution of overpressure in the North West Shelf, Australia, *Petroleum Exploration Society Australia*
587 *Journal* 28, 59-66.
- 588 Watson, D., Schofield, N., Jolley, D., Archer, S., Finlay, A. J., Mark, N., Hardman, J. & Watton, T. 2017.
589 Stratigraphic overview of Palaeogene tuffs in the Faroe–Shetland Basin, NE Atlantic Margin.
590 *Journal of the Geological Society, London*, **174**, 627–645.
- 591 Westbrook, G. K., and M. J. Smith. "Long decollements and mud volcanoes: Evidence from the Barbados Ridge
592 Complex for the role of high pore-fluid pressure in the development of an accretionary
593 complex." *Geology* 11.5 (1983): 279-283.
- 594 White, R. and McKenzie, D., 1989, Magmatism at rift zones: the generation of volcanic continental margins and
595 flood basalts. *Journal of Geophysical Research: Solid Earth*, 94(B6), pp.7685-7729

596
597

598 Nick Schofield is a Senior Lecturer in Igneous and Petroleum Geology at the University of
599 Aberdeen, where he leads the Atlantic Margin Research Group. He has published ~ 50 papers
600 on sill emplacement and the interaction of volcanism with petroleum systems. Nick has a PhD
601 from the University of Birmingham and a BSc(Hons) from the University of Edinburgh

602

603 Simon Holford is Associate Professor of Petroleum Geoscience at the University of Adelaide's
604 Australian School of Petroleum, where he co-leads the Stress, Structure & Seismic Research
605 Group. Simon has published ~90 papers on the prospectivity and tectonics of margins,
606 petroleum geomechanics and magmatism in basins. Simon has a PhD from the University of
607 Birmingham and a BSc(Hons) from Keele University.

608 Alex Edwards is the Global Portfolio Manager for Wells at Ikon Science, having joined in 2009.
609 He has been involved in all aspects of regional pore pressure analysis, pre- and post well
610 analysis. Alex received a MEdSci in geology (2005) from the University of Liverpool and a PhD
611 in structural geology at the University of Manchester.

612 Niall Mark completed his PhD in Interaction of Igneous Intrusions with Petroleum Systems in
613 2019. He received a MSc in Hydrocarbon Exploration from the University of Aberdeen in
614 2014 and a BSc(Hons) in Earth Science from Glasgow University in 2012.

615

616 Stefano Pugliese is Lead Geoscientist with Chrysaor in the UK. He received his BSc geology
617 degree from the University of St. Andrews and a Ph.D. in igneous geology from Kingston
618 University. His petroleum career began in Vietnam looking at fractured basement plays but
619 over the last decade, has focused on the traditional Cenozoic and Mesozoic plays of the
620 North Sea.

621

622
623
624
625
626
627
628
629
630
631
632
633
634
635
636
637
638
639
640
641
642
643
644
645
646
647
648
649
650
651
652
653
654
655
656
657
658
659
660
661
662

Acknowledgments

JX Nippon UK Ltd are thanked for PSDM seismic data used in this study. Well data is from the Common Access Database (CDA). IHS Kingdom Software and Schlumberger Petrel Software was used for seismic interpretation. Schlumberger Techlog was used for display of wireline and FMI data. We would like to thank Joe Cartwright, Richard Swarbrick, Clayton Grove and Stephen O'Connor for the constructive and helpful reviews and discussions of this manuscript. PGS are thanked for continued support of the research group at Aberdeen. Barry Katz is thanked for editorial guidance and input. Frances Whitehurst is thanked for editing advice.

Figure 1 - Tectonic elements of the Faroe-Shetland Basin. Adapted from Ellis et al. (2009), Mudge (2014), Watson et al. (2017) and Hardman et al. (2018a,b). Wells that contain evidence for overpressured intrusions are labelled. Map in Mercator/ED50 datum.

Figure 2 - Regional seismic line through well 214/28-1. Data courtesy of PGS – FSB MegaSurvey plus.

Figure 3 - Velocity vs. Density cross-plot for well 214/28-1. Examining velocity and density relationships can reveal information about the mechanism of overpressure development (Lahann et al., 2001 following the work of Bowers, 1994, 1995). The deepest shales (Cretaceous age) do not deviate from the Gardener shale trend, which is indicative of disequilibrium compaction as the sole pressure mechanism. The density values, however, exceed 2.45 g/cm³ (typical maximum density due to mechanical compaction) which suggests low porosity shales. The corrected bottom hole temperature (BHT) is 167°C (332°F) and therefore the high-density values correspond to diagenetic shale alteration.

Figure 4 - Seismic line through Well 214/28-1 located in the Faroe-Shetland Basin, offshore NW Scotland. The seismic line is from a 3D cube acquired 2011-2012 and reprocessed to Pre-Stack Depth Migration in 2016. The lower zone of intrusions, where overpressure was encountered (Fig. 5 and 6), extend in a down-dip direction towards a depth of ~ 6.5 km (21,325 ft).

Figure 5 - Pressure vs depth plot. Direct pressure data (e.g. RFT) from well 214/28-1 and well 214/27-1 (located 10 km away, that penetrated same stratigraphic succession).

663 **Figure 6** – Diagram showing log responses, static mud weight (MPa) and total gas from the lower zone of
664 intrusions where overpressure was encountered in well 214/28-1.
665

666
667 **Figure 7** – 2D seismic line (NS92202) across Well 219/28-2Z, showing inclined intrusion which was penetrated
668 at 3048 mBRT (~ 3.1 sec TWT).
669

670
671 **Figure 8** – Detail of a sill penetrated at 3148 mBRT. An RFT measurement taken at the sill edge recorded a
672 pressure of 48 MPa (6,956 Psi), some 8 MPa (1,160 Psi) higher than the surrounding sequences. This pressure
673 was equivalent to that recorded in RFT measurements at the base of the well (see main text for details). This
674 suggests that the sill penetrated at 3148 mBRT (10,328 ft BRT) was in pressure communication with deeper
675 units.
676

677 **Figure 9** – Pressure vs. Depth plot for well 219/28-2Z
678

679
680 **Figure 10** - Wireline and FMI log through a 27 m (88 ft) thick igneous intrusion located within the Faroe-
681 Shetland Basin (213/27-2). Clear fractures can be observed within the intrusion on the FMI log. We interpret
682 the sub-vertical fractures, which extend $>30^\circ$ around the circumference of the hole, to be primary cooling
683 fractures and not drilling induced, as no sub-vertical fractures are seen in the weaker shales horizons above and
684 below the intrusion, and no change in mud weight occurred while drilling from the shale through to the intrusion.
685 Note the increased separation of the Deep and Medium Resistivity wireline measurements within the heavily
686 fractured area of the intrusion (from 3270 m down), and how this separation is greatly reduced within the zone
687 of minimal fracturing towards the top of the intrusion and within the claystone sequence.

688
689 **Figure 11** – Seismic Line through the 6.1 m (20 ft) thick intrusion penetrated by 214/28-1, highlighting the
690 continuous path that that can be traced vertically and horizontally through the intrusive body from point of
691 intersection at 4,596 mBRT (15,078 ft BRT) to a larger intrusive complex at depths >6 km (~ 20,000 ft).
692

693 **Figure 12 A)** Diagram showing concept of the Centroid, which is commonly used to explain overpressure
694 within sand bodies as a result of becoming inclined post-deposition (see Traugott and Heppard, 1994; Swarbrick
695 and Osborne, 1998) **B)** The modified concept of lateral drainage through a fractured intrusion. It is important
696 to note that unlike the concept of the centroid, which relies on recent tilting of the sand body to produce
697 differential pressures, in the case of intrusions, it is their cross-cutting and tendency to intrude sub-vertically
698 which leads to the pressure transfer and drainage, if connected at depth to more overpressured units.
699

700 **Figure 13** - Conceptual diagram showing the principle of pressure transmission through a fractured igneous
701 intrusive complex. Such a process can lead to overpressure being transferred laterally (and vertically) through a
702 basin 10s of km away from its point of origin.
703

704

705

706

707

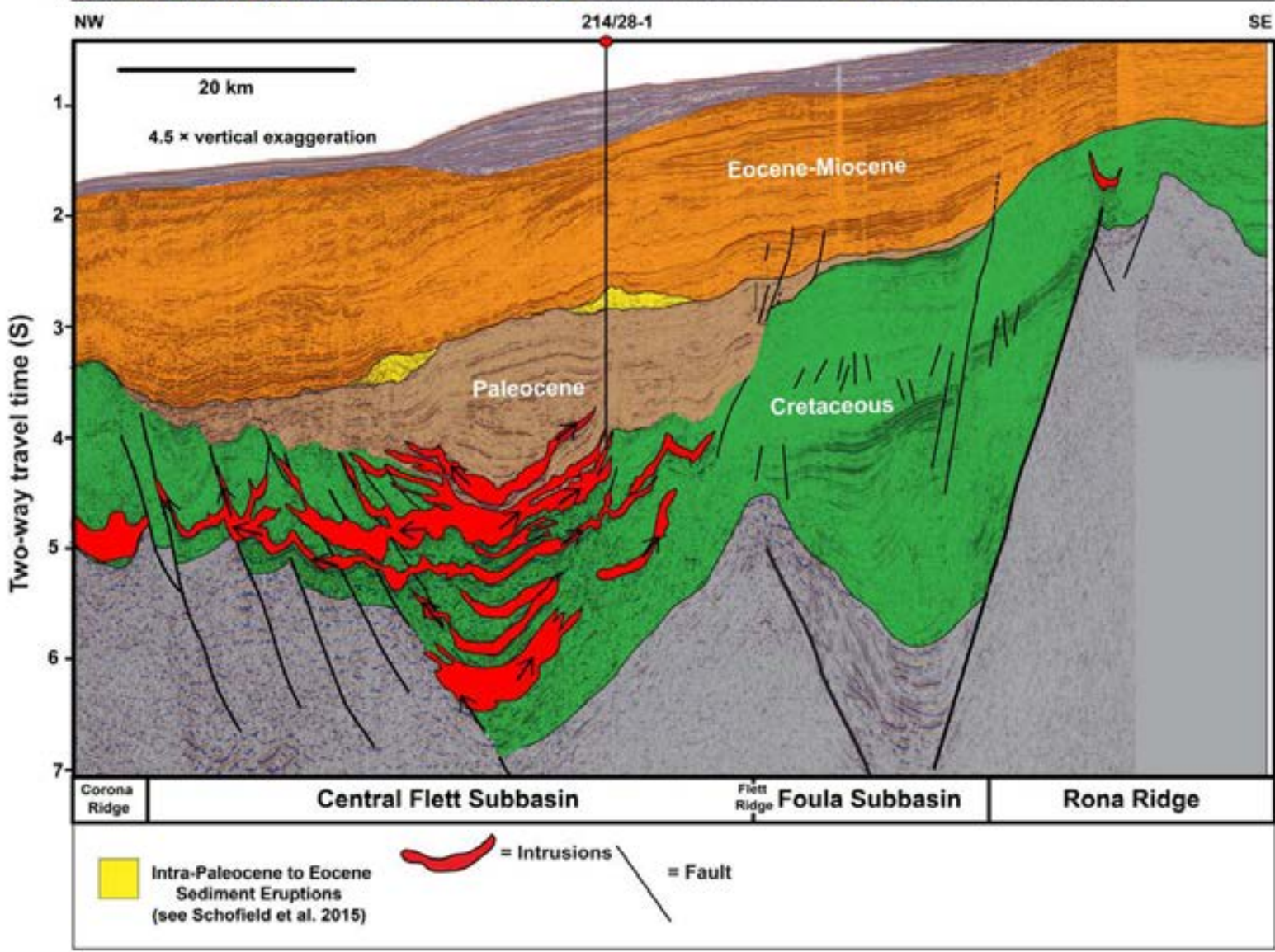
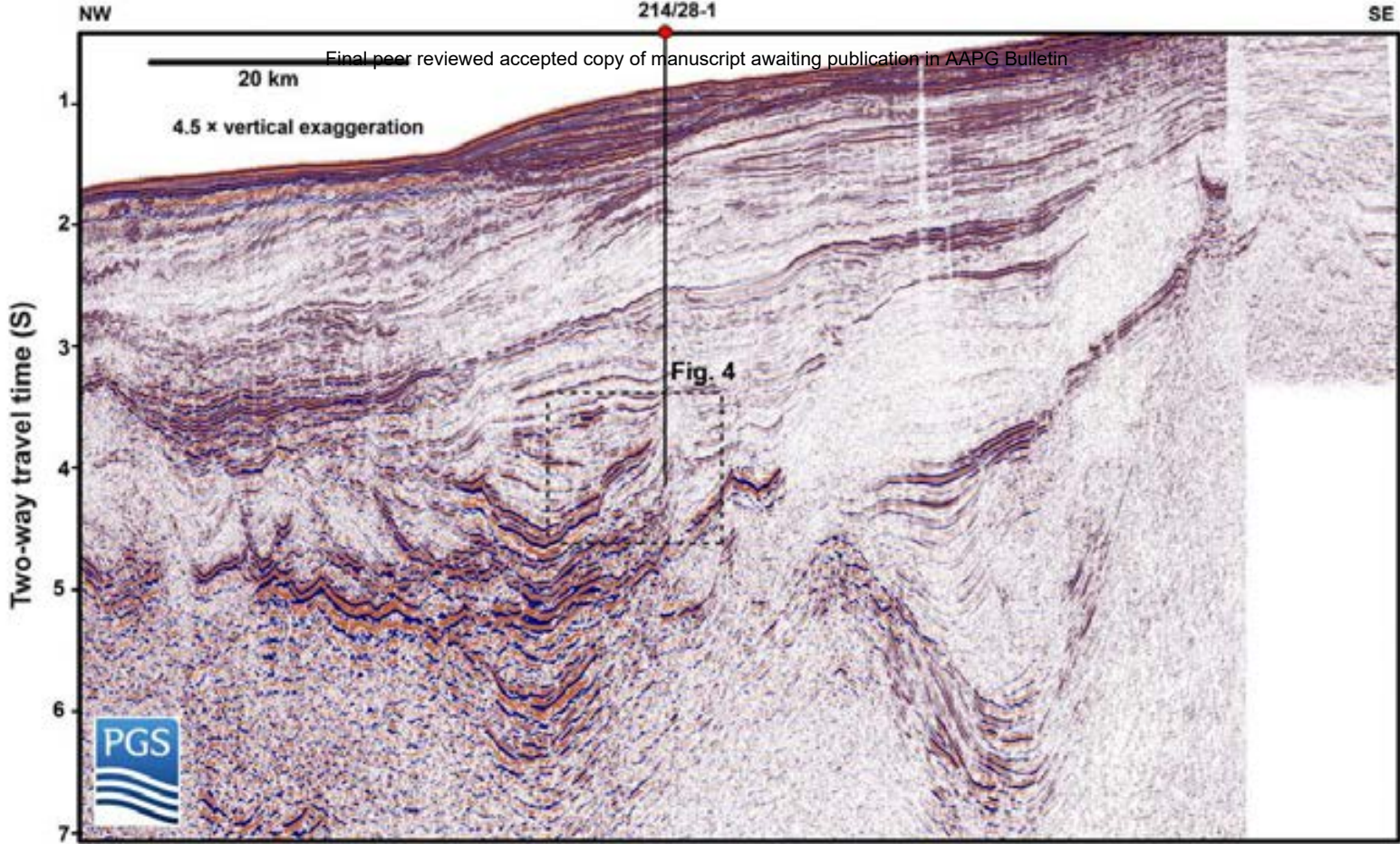
708

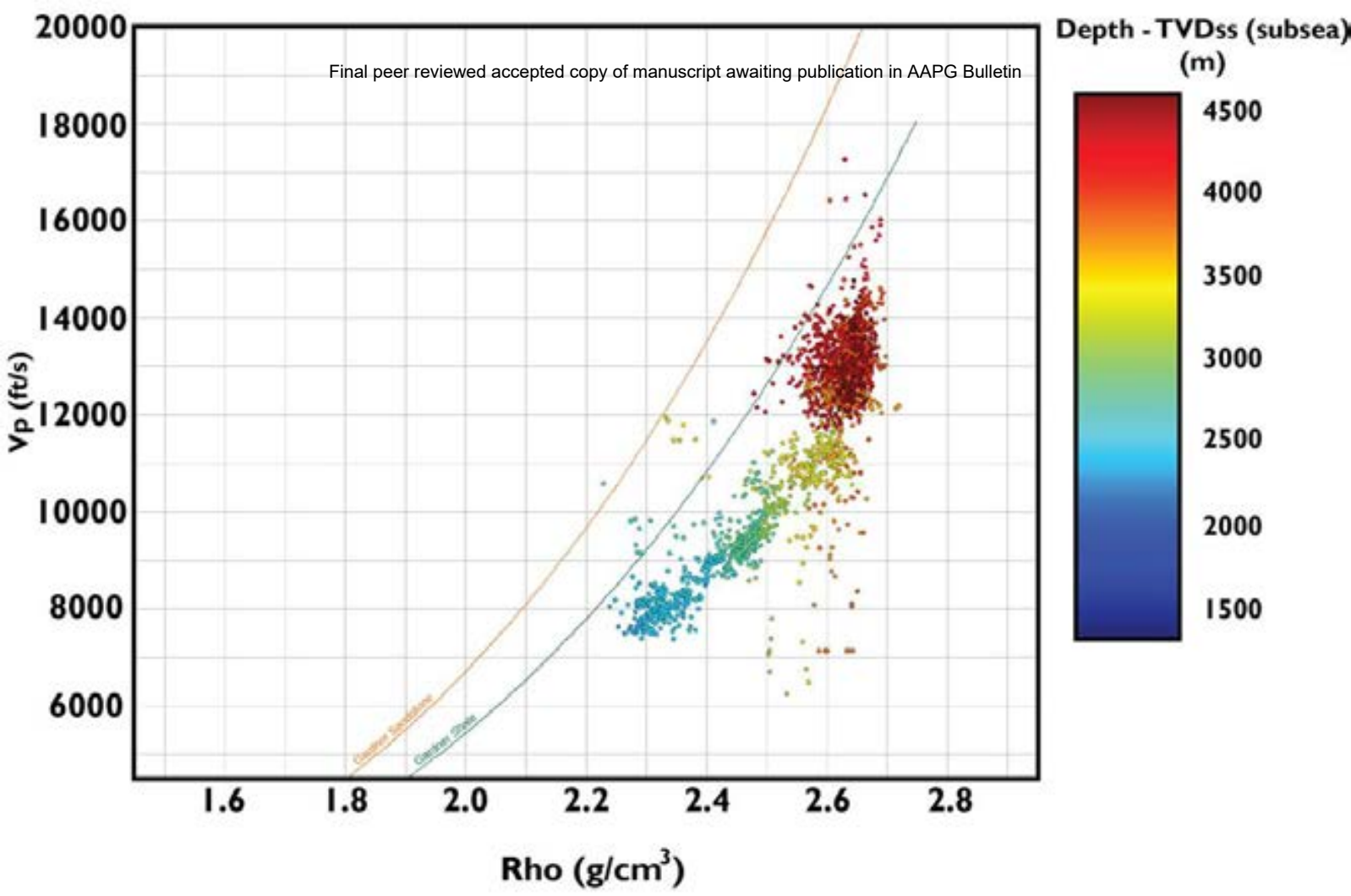
709

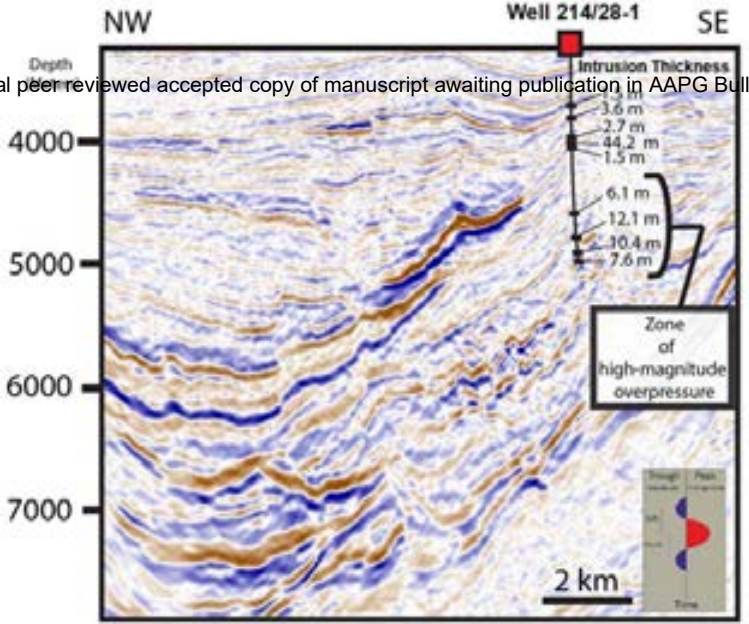
710

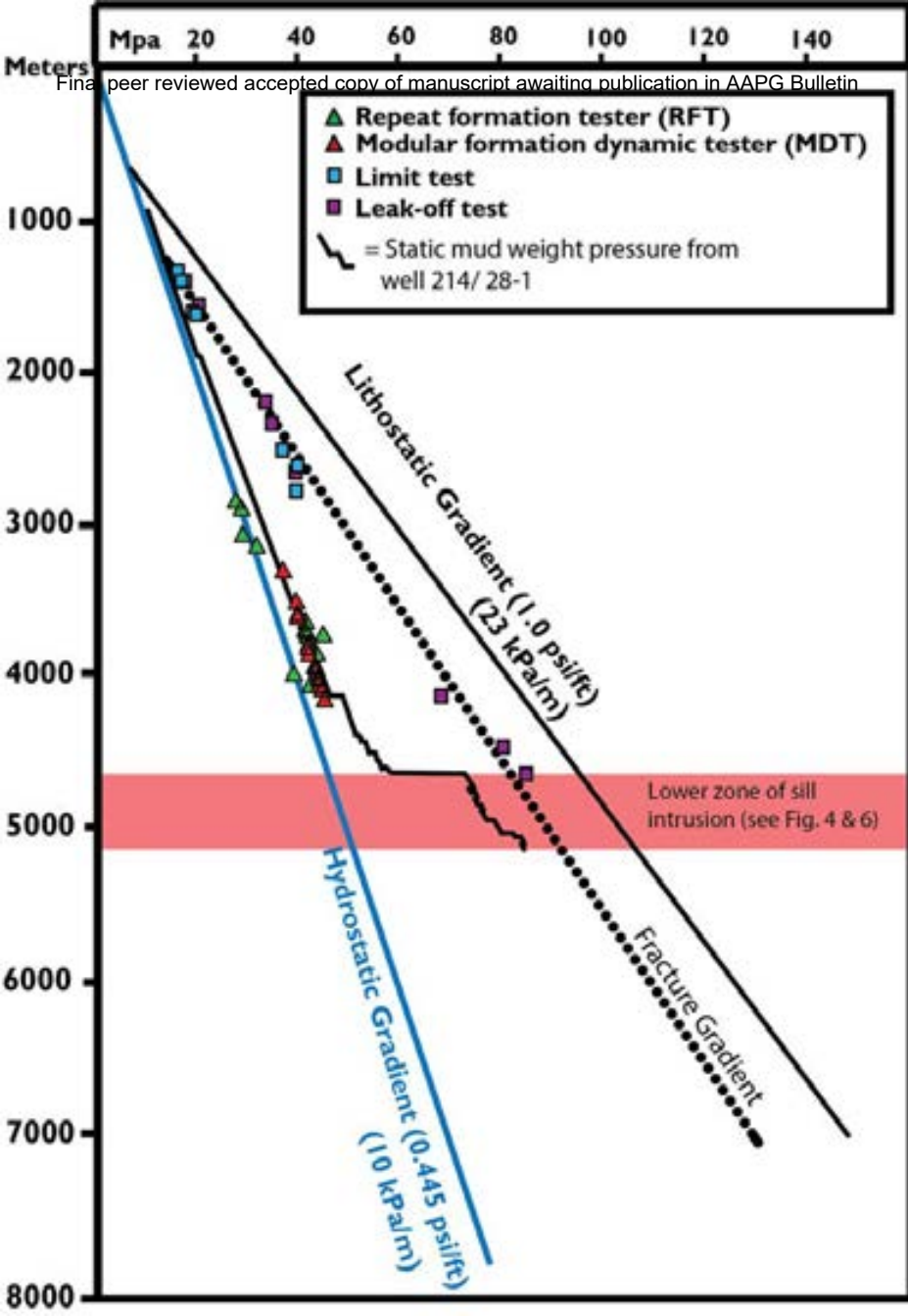
711

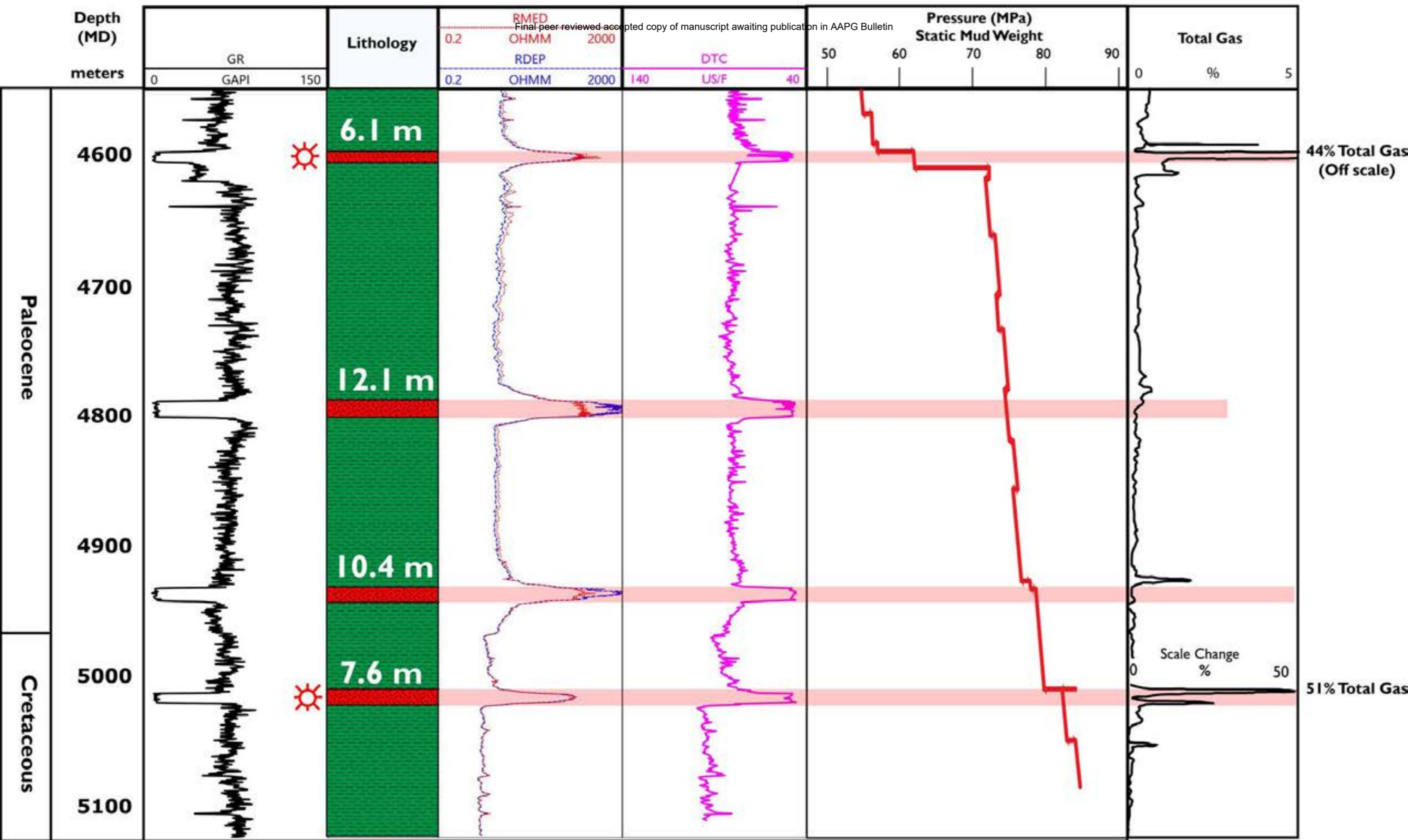
712

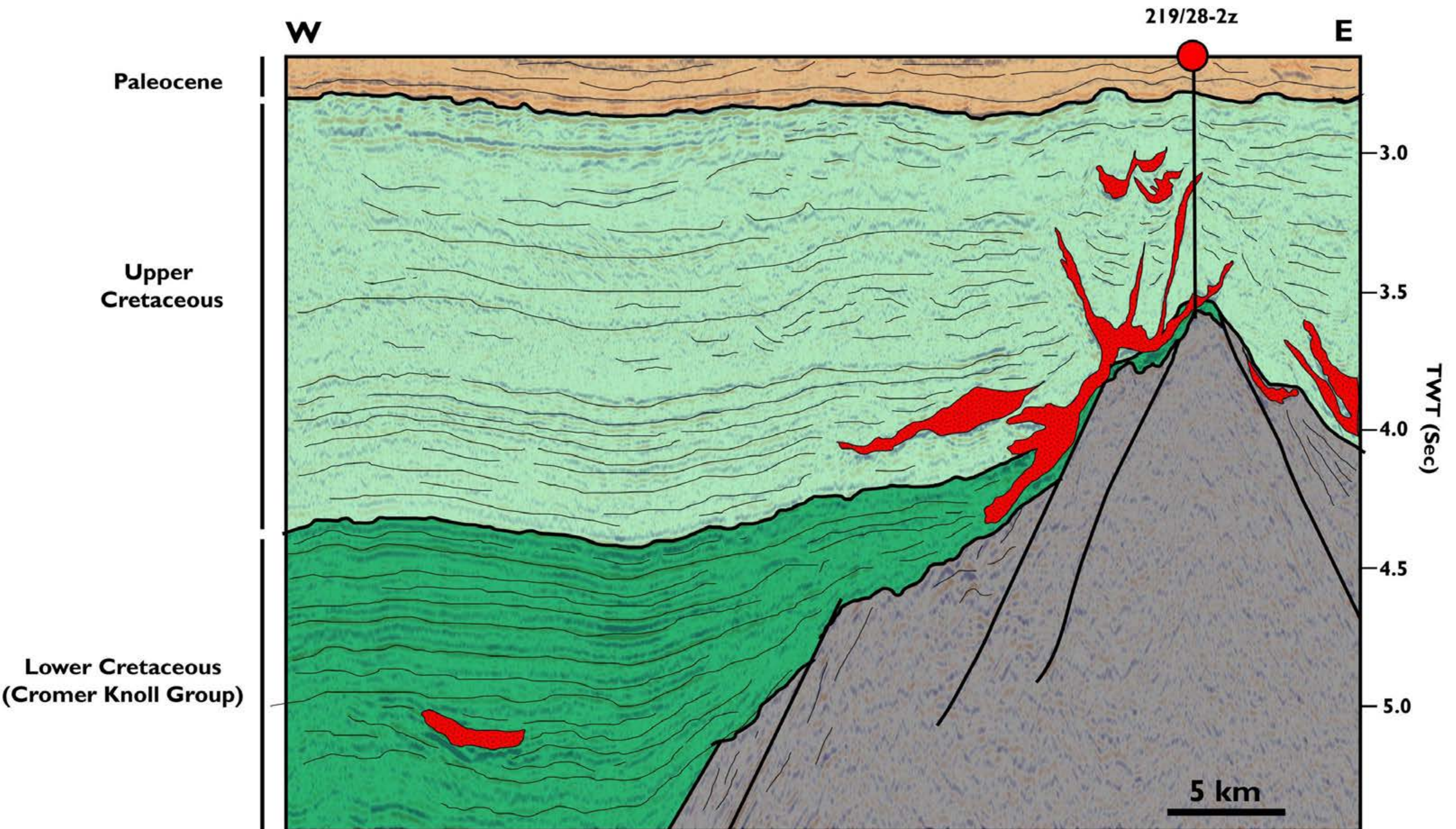
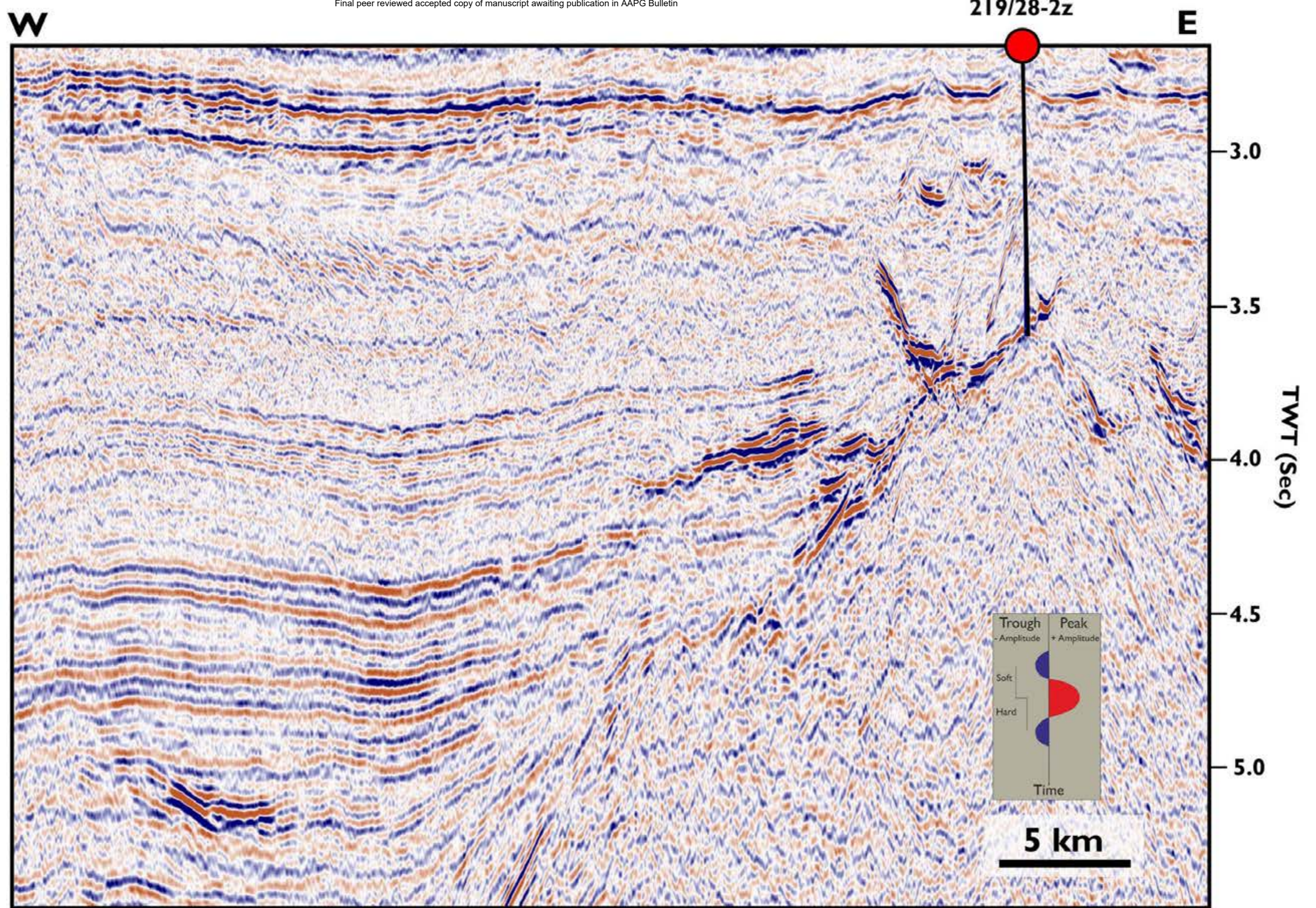


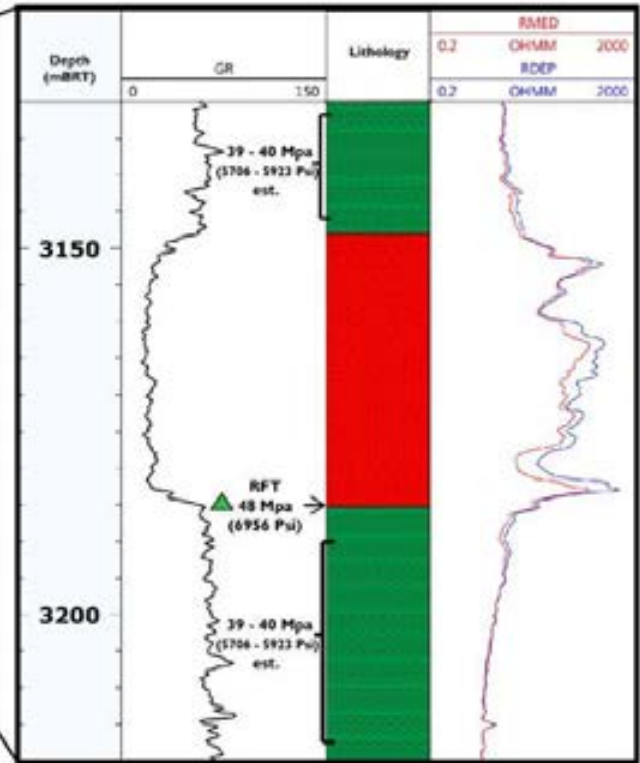
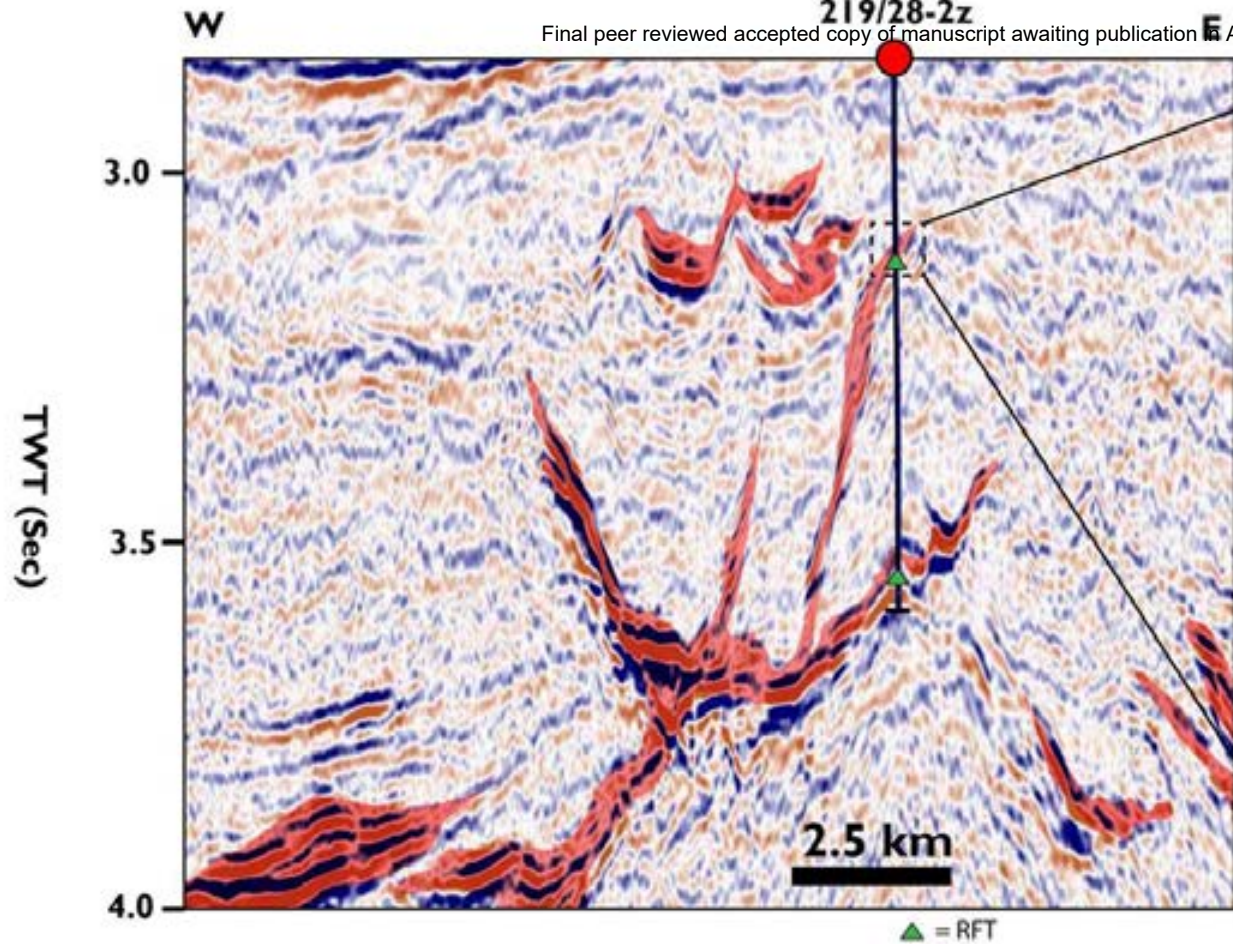


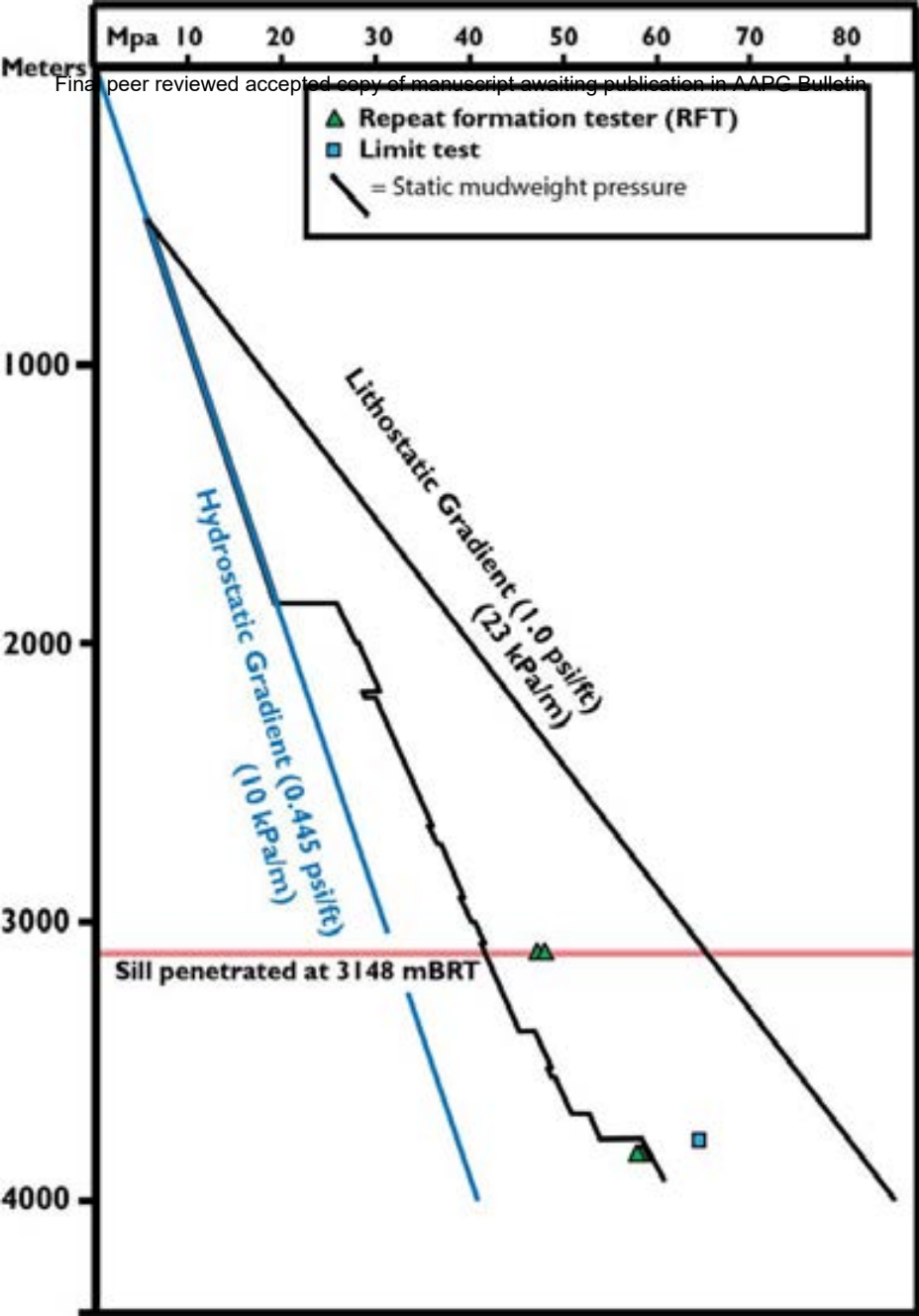


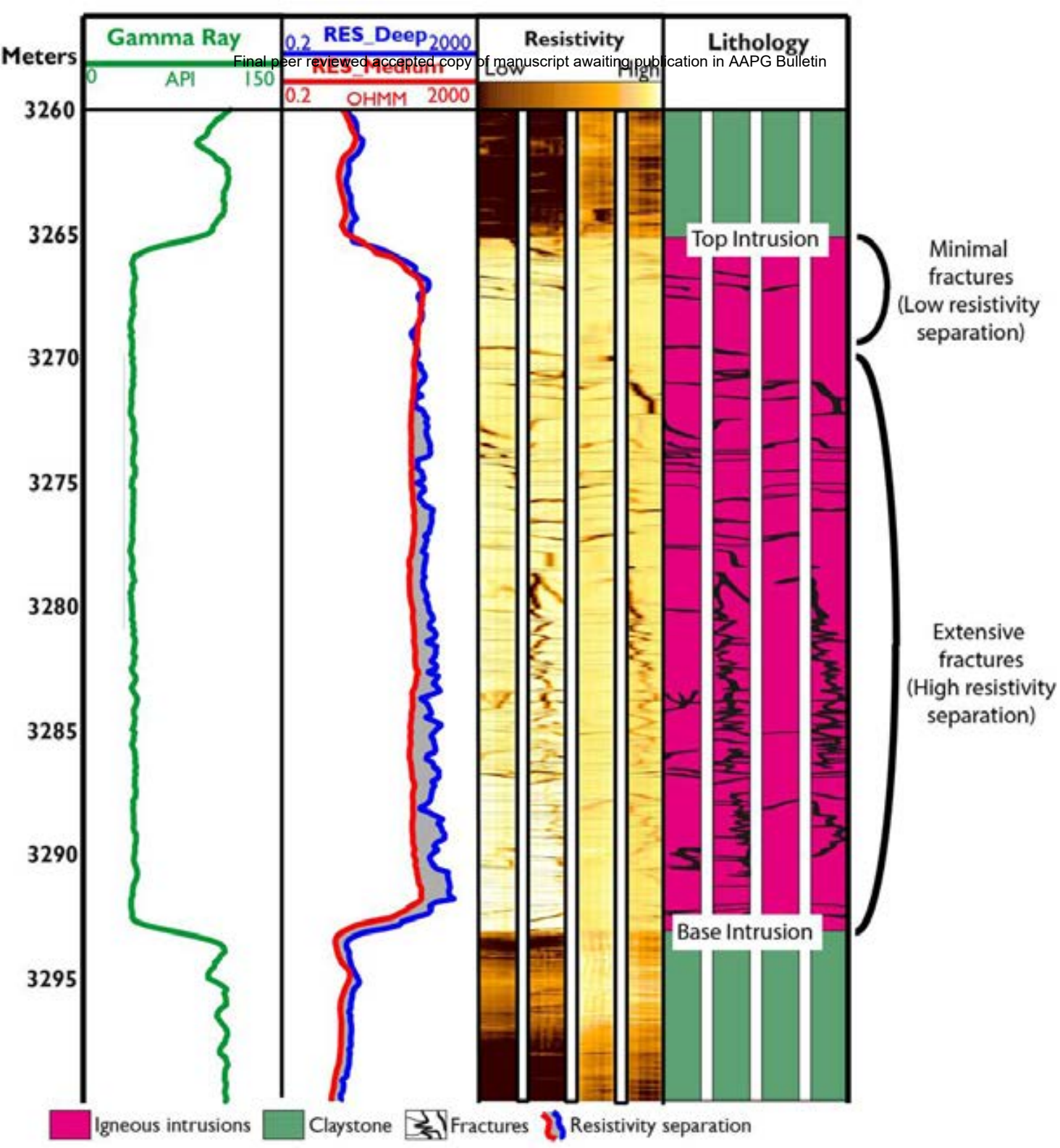




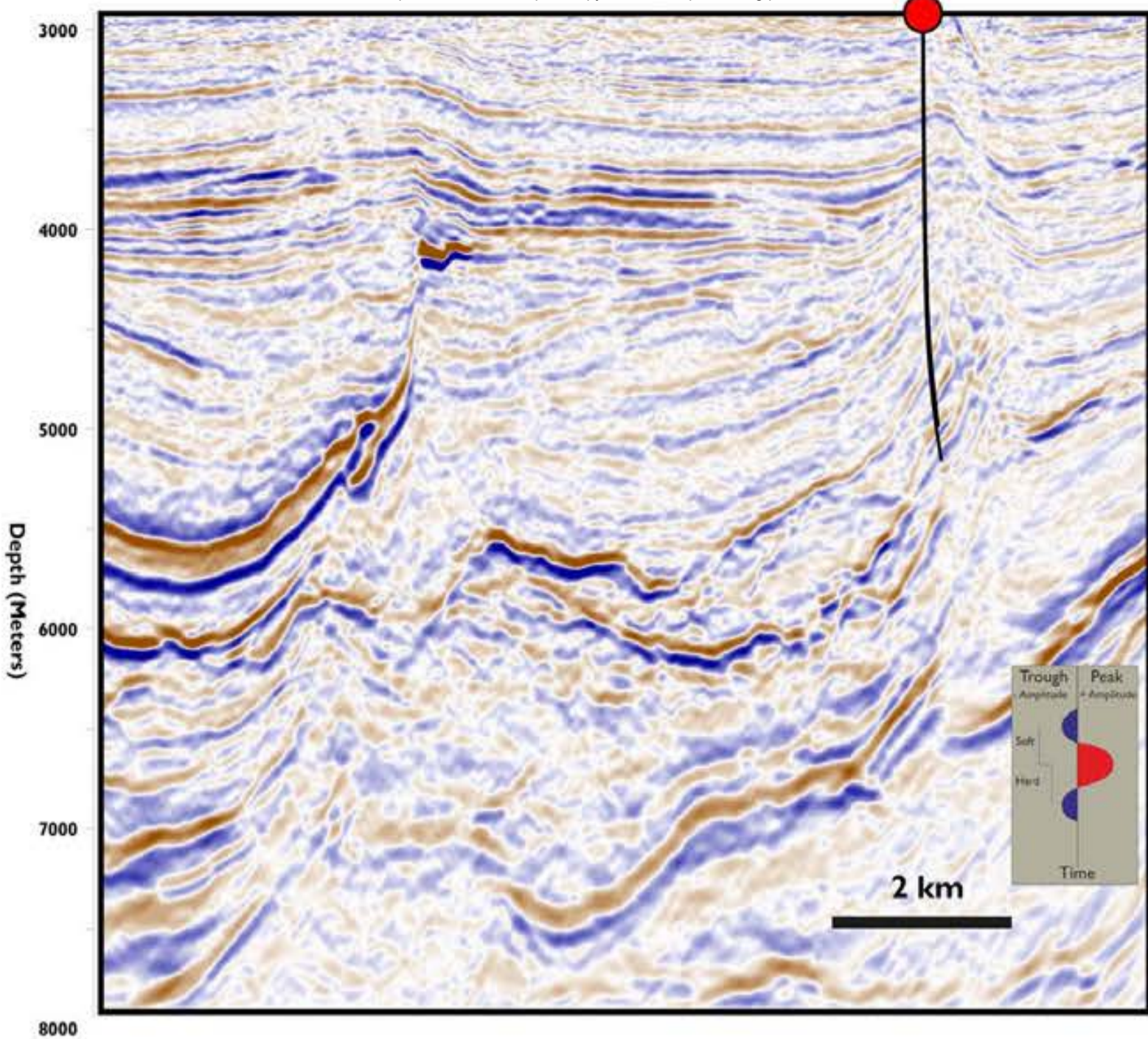




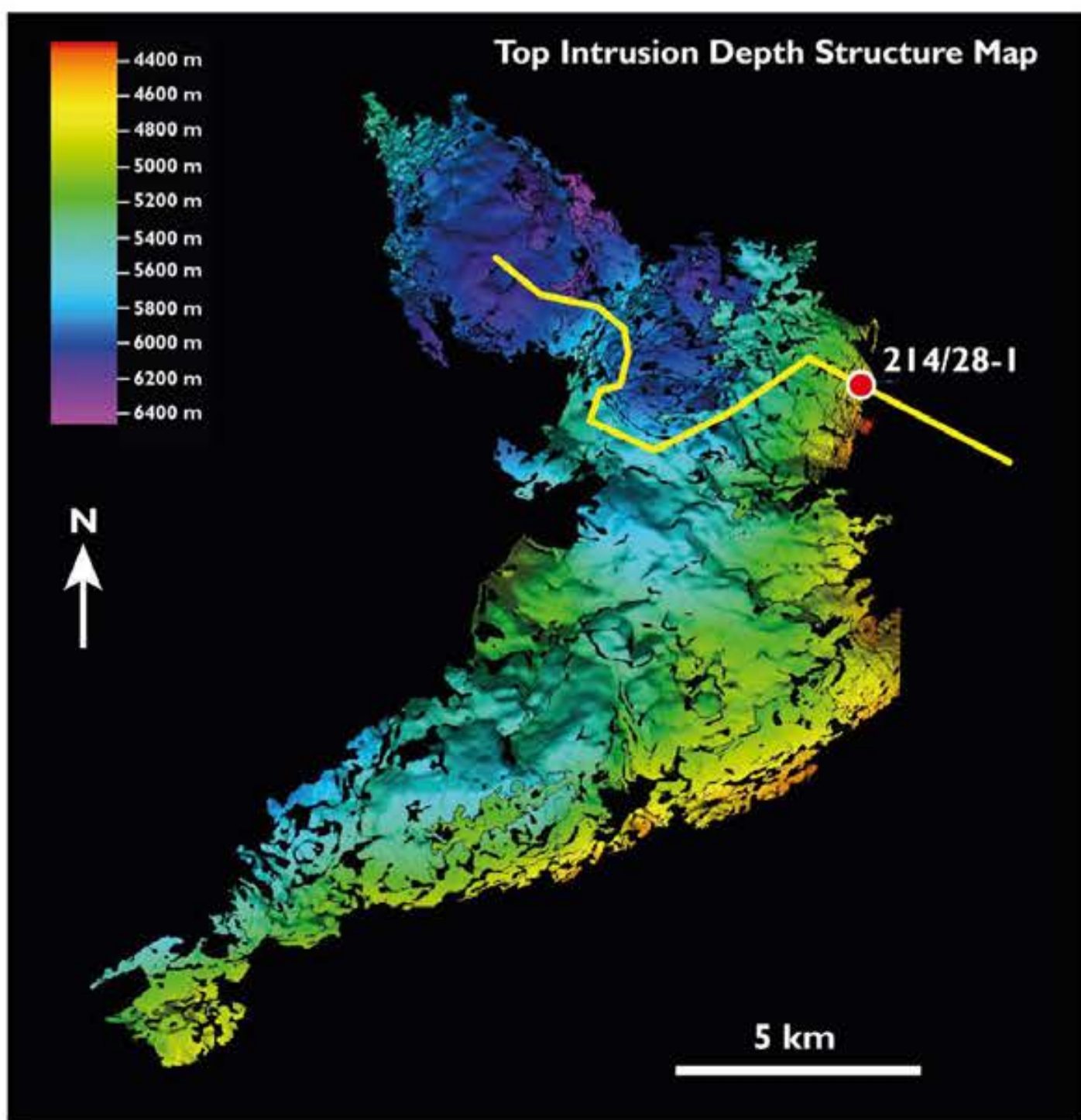
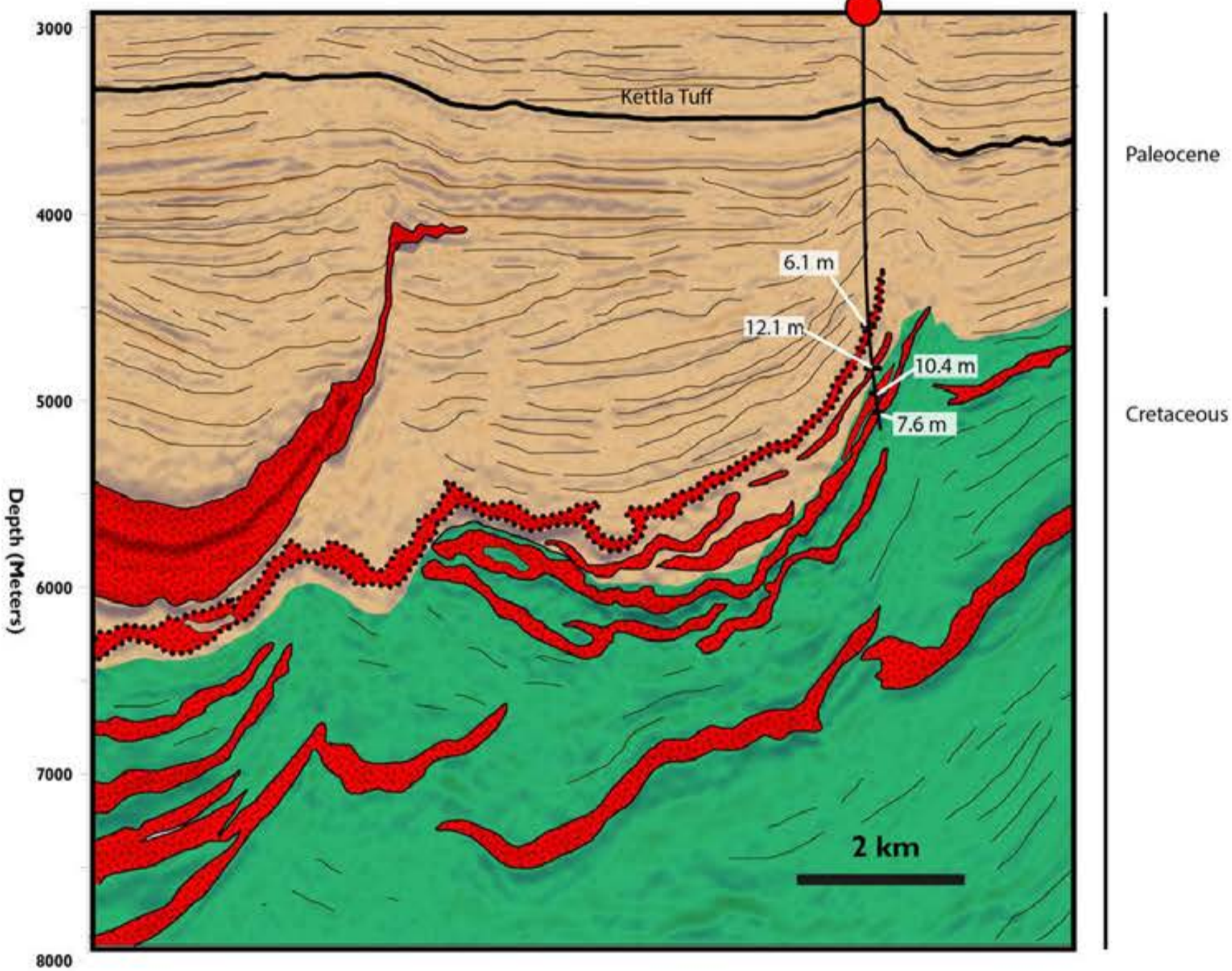




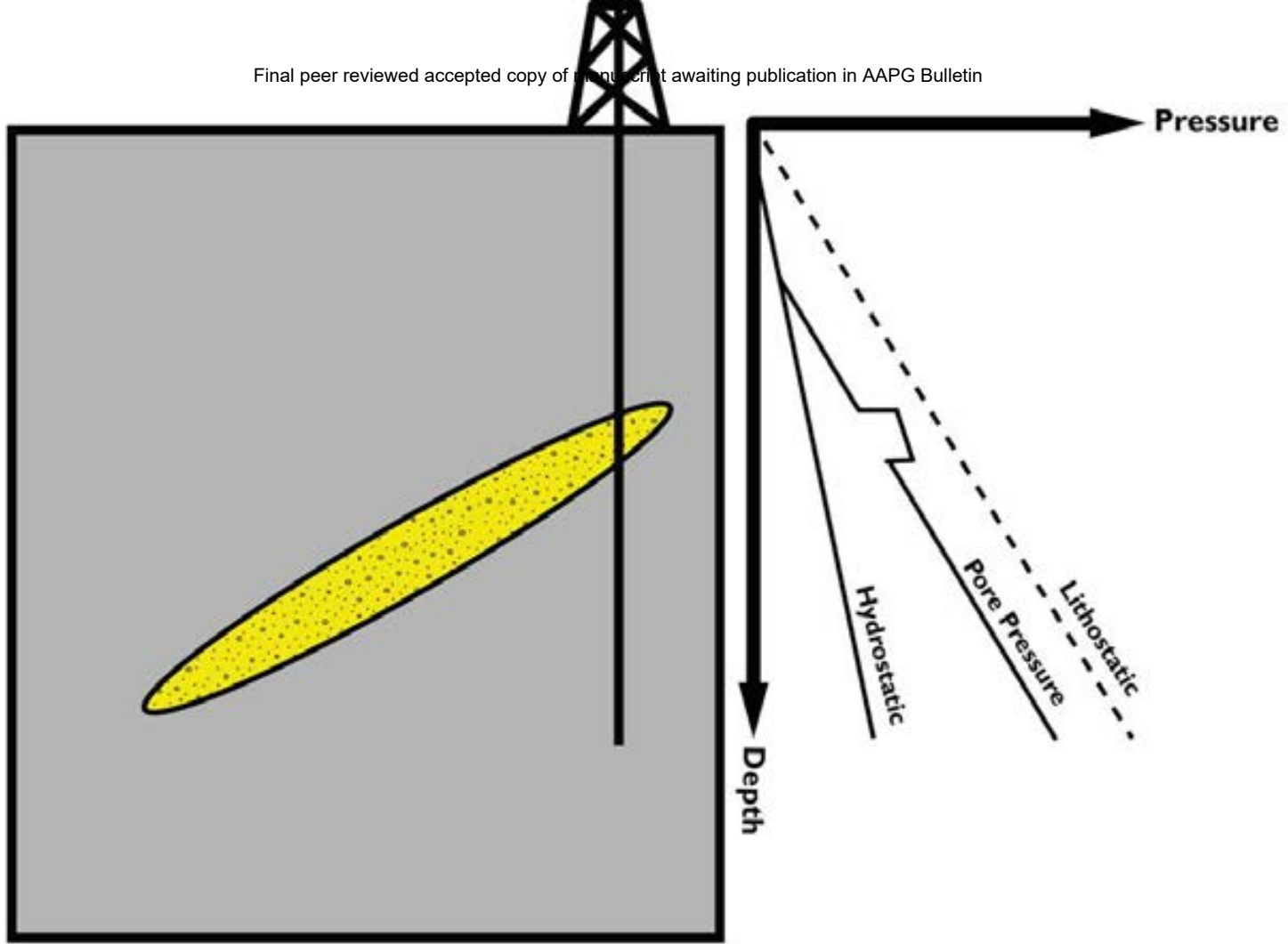
214/28-1



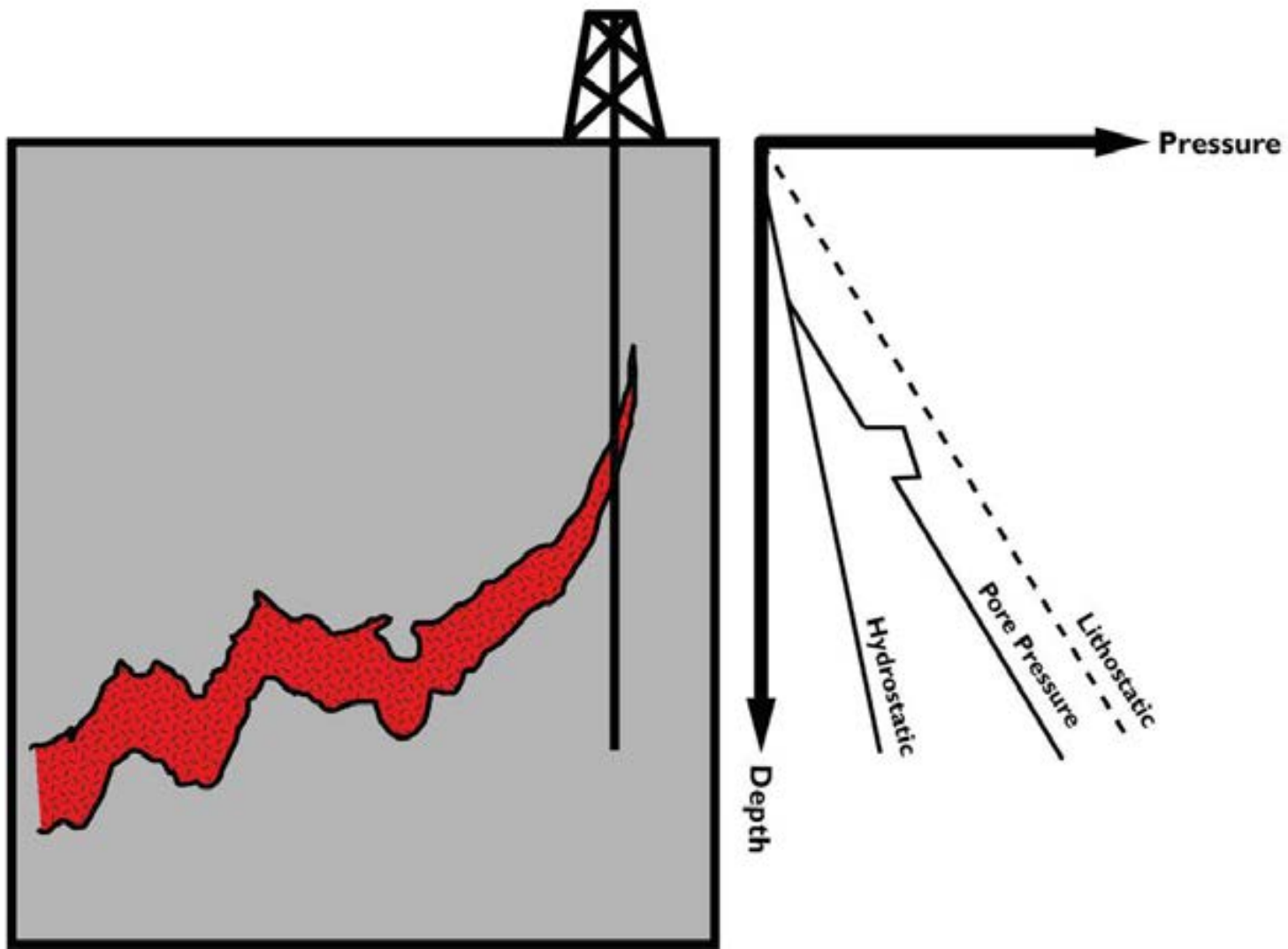
214/28-1



A)



B)



Sea Surface



Final peer reviewed accepted copy of manuscript awaiting publication in AAPG Bulletin

Pressure →



= Pressure transmission route through interconnected fractured intrusions

Depth ↓

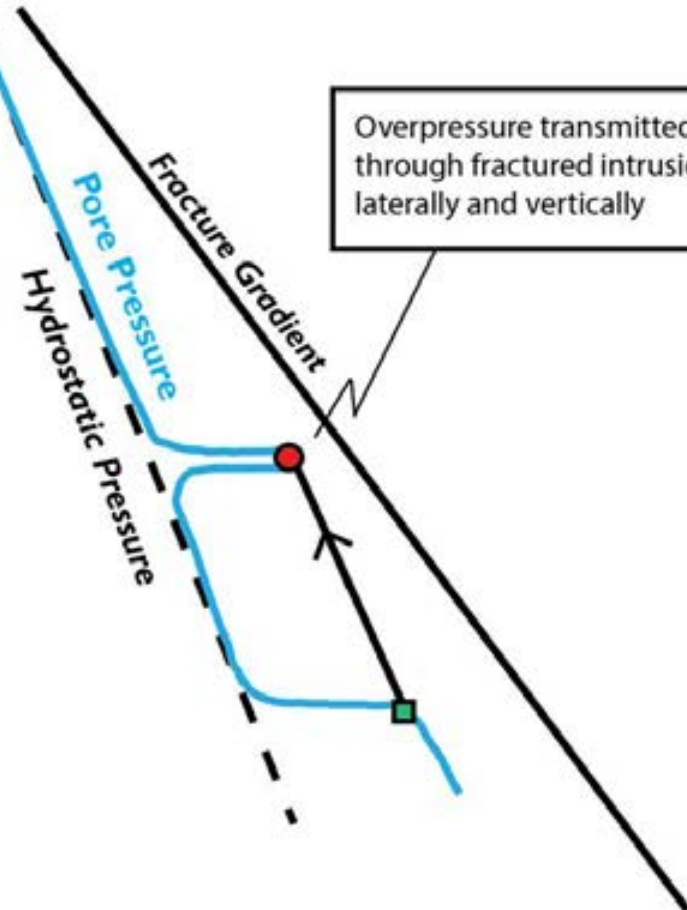
Low



Pore-Pressure

High

Overpressured Sequence



Overpressure transmitted through fractured intrusions laterally and vertically